2mic

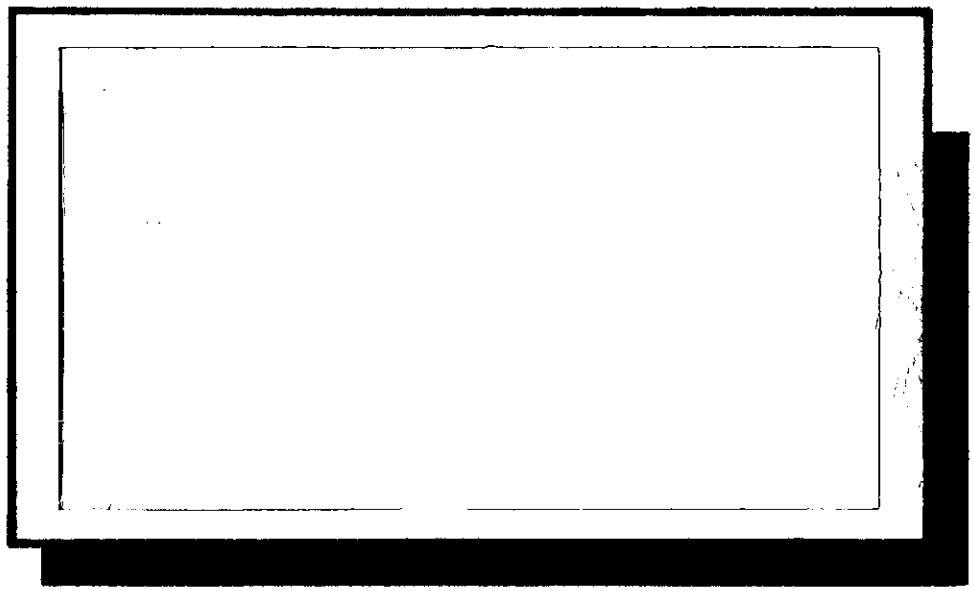

CENTER FOR SPACE RESEARCH

MASSACHUSETTS INSTITUTE OF TECHNOLOGY

This work was supported in part by the National Aeronautics and Space Administration under Grant NGL 22-009-372.

STELLAR WINDS DRIVEN BY ALFVÉN WAVES

by

John W. Belcher and Stanislaw Olbert

CSR TR-73-5 October, 1973

Department of Physics and Center for Space Research
Massachusetts Institute of Technology
Cambridge, Massachusetts 02139

ABSTRACT

We consider models of stellar winds in which the dynamic expansion of a corona is driven by Alfvén waves propagating outward along radial magnetic field lines. In the presence of Alfvén waves, a coronal expansion can exist for a broad range of reference conditions which would, in the absence of waves, lead to static configurations. Wind models in which the acceleration mechanism is due to Alfvén waves alone exhibit lower mass fluxes and higher energies per particle as compared to wind models in which the acceleration is due to thermal processes. For example, winds driven by Alfvén waves exhibit streaming velocities at infinity which may vary between the escape velocity at the coronal base and the geometrical mean of the escape velocity and the speed of light. We derive upper and lower limits for the allowed energy fluxes and mass fluxes associated with these winds.

CONTENTS

I. INTRODUCTION

The properties of stellar winds which are thermally driven have been the subject of extensive theoretical investigation over the last fifteen years. Dynamical models of such winds have become increasingly sophisticated, including effects due to the two fluid nature of the plasma, magnetic fields and stellar rotation, the inhibition of thermal conductivity, the propagation and damping of hydromagnetic waves in the expanding solar corona, and many others. For comprehensive reviews of these topics, see the articles by Parker (1971) and Barnes (1973), or the book by Hundhausen (1972).

Recently, Belcher (1971, 1972), and, independently, Alazraki and Couturier (1971) have considered modifications of polytrope wind models due to the presence of undamped Alfvén waves propagating outward along radial magnetic field lines. The interaction of the waves with the streaming plasma produces an outward pressure gradient, analogous to that of a radiation pressure, which results in a radial acceleration of the wind. In this manner, undamped wave energy fluxes propagating outward into an expanding corona are completely transformed into enhanced streaming energy fluxes of the wind at large distances from the star. Parker (1965) was the first to suggest that undamped Alfvén waves could affect the dynamics of the solar wind. However, detailed considerations of the problem were not undertaken until observational evidence suggested that Alfvén waves generated close to the sun are in fact present

at 1 a.u. (Coleman 1967, Unti and Neugebauer 1968, Belcher et al. 1969, Belcher and Davis 1971). Since the original one fluid treatments, various authors have also considered the effects of Alfvénic wave pressures in two fluid models (Hollweg 1973a), the modifications due to non-WKB terms in one fluid models (Hollweg 1973b), and the effects of finite and large amplitude Alfvén waves in one fluid models (Whang 1973, Barnes and Hollweg 1973). Hollweg (1972) has also considered possible generation mechanisms for these waves in the solar chromosphere.

For obvious historical reasons, the initial treatments of wave pressures are primarily concerned with situations in which the Alfvén wave energy flux across the base of the corona is less than the conductive flux of thermal energy - that is, the addition of wave pressures is considered to be a modification of an essentially thermal process. In the opposite extreme, however, Alazraki and Couturier (1971) point out that wind solutions to the equations of motion always exist as long as the wave energy flux is non-zero, even if the conductive flux of thermal energy is identically zero. Such wave driven winds may exhibit large energies per particle at infinity, in conjunction with small mass fluxes (Belcher 1971). It is thus possible for Alfvén waves alone to drive a coronal expansion, and the properties of winds produced in this manner may be very different from those of thermally driven winds. In the present paper, we investigate in detail the characteristics of stellar winds which are primarily driven by low-frequency, outwardly-propagating Alfvén waves generated close to a star. The thermal

properties of the plasma are represented by a polytrope relation between density and pressure, and we consider only thermal parameters which in the absence of waves would result in static atmospheres. For a given set of initial parameters (wave strengths, temperatures, densities, and so on) at some reference level close to the star, we wish to determine whether or not the dynamical expansion of the atmosphere into a stellar wind is possible, and, if so, to ascertain the mass and energy fluxes associated with that wind. We assume that all generation mechanisms for the Alfvén waves (e.g., convective zones) occur inside the reference level, and that there is no damping of the waves external to the reference level. As we shall see, there are a broad range of wind solutions possible.

Before proceeding with the detailed mathematics, we offer some rationale for the formulation we use. First, to keep the calculation tractable, we consider only radial streaming in the presence of a radial magnetic field, with no stellar rotation. Second, the winds we shall encounter may exhibit rapid decreases in mass density outward from the reference level, whereas the magnetic field strength decreases less rapidly, as $1/r^2$. Consequently, the Alfvén velocity in the low density, field dominated plasma may be high, and we must insure that it does not exceed c, the speed of light. As we shall show, the fact that both Alazraki and Couturier (1971) and Belcher (1971) allow the Alfvén velocity to be arbitrarily large invalidates their results at low mass fluxes. Third, in some limits we shall encounter winds with arbitrarily large energies per particle

far from the star, in conjunction with very low mass fluxes. Although the physical validity of these solutions is questionable, we must allow for the possibility of relativistic streaming velocities at infinity to handle the limits properly. Finally we shall find circumstances in which wind solutions formally exist even for tightly bound atmospheres near massive objects with high escape velocities. Thus our initial approach should allow for escape velocities, Alfvén velocities, and radial streaming velocities which may be comparable to the speed of light. We consider only situations in which the local sound velocity and the transverse velocity perturbation associated with the wave are small compared to the speed of light. To insure the validity of our relativistic limits, and for the rigor and novelty of the approach, we derive our basic wind equations using the covariant formulation of magnetohydrodynamics. For the reader unfamiliar with this formalism, we sketch in an appendix the derivation of the non-relativistic limits of our equations, using the more familiar descriptions of MHD.

II. MATHEMATICAL FORMULATION

a) The Covariant Equations of Motion

We consider the relativistic magnetohydrodynamic equations appropriate for an ionized, highly conducting fluid in the presence of electromagnetic fields, following closely the formulation of Greenberg (1971). The space-time metric tensor $g_{\mu\nu}$ (Greek indices take the values 0, 1, 2, 3) is defined such that

$$ds^2 = g_{\mu\nu}\, dx^\mu\, dx^\nu \tag{II.1}$$

with the contravariant four-velocity given by

$$U^\mu = \frac{dx^\mu}{ds} \qquad \text{with} \quad U^\mu\, U_\mu = +1 \tag{II.2}$$

We take the coordinates (x^0, x^1, x^2, x^3) to be (ct, r, θ, ϕ) in the usual spherical polar sense, and assume that the metric tensor $g_{\mu\nu}$ is determined solely by the presence of a spherically symmetric body of mass M. If G is the gravitational constant and c the speed of light, then we define the "escape velocity" $c\beta_e$ such that

$$\beta_e^{\,2} = \frac{2GM}{rc^2} \tag{II.3}$$

and we take

$$\eta = 1 - \beta_e^{\,2} \tag{II.4}$$

We choose the Schwarzschild metric: $g_{00} = \eta$, $g_{11} = -1/\eta$, $g_{22} = -r^2$, $g_{33} = -r^2\sin^2\theta$, and $g_{\mu\nu} = 0$ for $\mu \neq \nu$.

The antisymmetric electromagnetic field tensor $F_{\mu\nu}$ is (cf. Landau and Lifshitz, 1971, Chapter 10)

$$F_{i0} = - E_i \qquad F_{12} = - \frac{H_3}{\eta \sin \theta}$$

$$F_{13} = + \frac{H_2 \sin \theta}{\eta} \qquad F_{23} = - H_1 r^2 \sin \theta \tag{II.5}$$

where E^i and H^j are space vectors (Latin indices take only the values 1, 2, 3). The three-dimensional metric tensor is $- g_{ik}$. If J^μ is the four-current density, and g is the determinant of the tensor g_{ik}, then Maxwell's equations have the form

$$\frac{\partial F_{\mu\nu}}{\partial x^\lambda} + \frac{\partial F_{\lambda\mu}}{\partial x^\nu} + \frac{\partial F_{\nu\lambda}}{\partial x^\mu} = 0 \tag{II-6a}$$

$$\frac{1}{\sqrt{-g}} \frac{\partial}{\partial x^\mu} \left[\sqrt{-g} \; F^{\nu\mu} \right] = - \frac{4\pi}{c} J^\nu \tag{II-6b}$$

The electromagnetic energy-momentum tensor $S_\mu{}^\nu$ is given by

$$S_\mu{}^\nu = \frac{1}{4\pi} \left[- F_{\mu\lambda} F^{\nu\lambda} + \frac{1}{4} \delta_\mu{}^\nu F_{\sigma\lambda} F^{\sigma\lambda} \right] \tag{II.7}$$

We take p to be the isotropic pressure of the fluid, ε to be the rest energy density of the fluid, and ρ^* to be the local rest mass density. The stress-energy tensor $T^{\mu\nu}$ for a fully ionized fluid in the presence of an electromagnetic field is

$$T^{\mu\nu} = (\varepsilon + p)\ U^{\mu}\ U^{\nu} - p g^{\mu\nu} + S^{\mu\nu} \tag{II.8}$$

The equation of motion of the fluid is

$$T^{\mu\nu}{}_{;\nu} = 0 \tag{II.9}$$

Following Greenberg (1971), we use the expression for $T^{\mu\nu}$ given by equation (II.8) to write the space components of equation (II.9) as

$$(\varepsilon + p)\ U^{\lambda}\ U^{\mu}{}_{;\lambda} = h^{\mu\sigma}\ \frac{\partial p}{\partial x_{\sigma}} - \frac{1}{4\pi}\ h^{\mu\sigma}\ F_{\sigma\nu}\ F^{\nu\lambda}{}_{;\lambda} \tag{II.10}$$

where

$$h^{\mu\nu} = g^{\mu\nu} - U^{\mu}\ U^{\nu}$$

The equation of continuity of rest-mass takes the form

$$(\rho^{*}\ U^{\nu})_{;\nu} = 0 \tag{II.11}$$

If ρ_e^{*} is the local charge density and σ the electrical conductivity of the fluid, then the invariant form of Ohm's law in magnetohydrodynamics is

$$J^{\nu} = \rho_e^{*}\ U^{\nu} - \sigma\ F^{\nu\lambda}\ U_{\lambda} \tag{II.12}$$

We will assume that σ is sufficiently large that the electric field in the co-moving frame is essentially zero; that is, we make the assumption that

$$U^{\mu}\ F_{\lambda\mu} = 0 \tag{II.13}$$

With this assumption, the local joule heating is zero, and we

may take a polytrope relation between p and ρ^*

$$p \propto (\rho^*)^{\alpha} \tag{II.14}$$

The time component of equation (II.9) implies that the energy density ε is given by [cf. equation (15) of Greenberg]

$$\varepsilon = \rho^* c^2 + \frac{p}{\alpha - 1}$$

If we define $c\beta_s$ to be the local speed of sound, then

$$\beta_s^2 = \frac{\alpha p}{\rho^* c^2} \tag{II.15}$$

and we find that

$$\varepsilon + p = \rho^* c^2 \left(1 + \frac{\beta_s^2}{\alpha - 1}\right) \tag{II.16}$$

Equations (II.1) - (II.16) represent the basic set of fluid equations for collisionless plasma. We shall now specialize these equations to the problem at hand.

b) Radial Dependence of Wave Amplitudes in the WKB Approximation

We seek solutions to the above equations which exhibit steady-state radial streaming, a radial background magnetic field, and time-dependent transverse fluctuations in field and velocity which are locally Alfvénic and outwardly-propagating. Our procedure is as follows. We decompose our covariant equations into radial components and components transverse to the radial. The eikonal (or WKB) method (Weinberg 1962) is applied to the transverse equations to obtain the local

dispersion relation and the wave amplitudes as functions of radius, density, radial velocity, and radial magnetic field. Once these expressions are known, we can write the radial component of the momentum equation and the conserved energy flux equation as functions of radius, density, and radial velocity alone.

In this section, we find the local wave amplitudes using the short-wavelength approximation, often referred to as the WKB approximation. We initially assume that the Alfvén waves are linearly polarized in the ϕ-direction, and then generalize our results to the case of circular polarization. From Møller (1952, Chapter X), we may write the four-velocity U^μ of the plasma as

$$U^\mu = \Gamma(1,\ \beta,\ 0,\ \frac{\delta\beta}{r \sin\theta})$$

where $c\beta$ is (dx^1/dt) and thus represents the contravariant component of the radial spatial velocity; $c\delta\beta$ is the transverse velocity, and

$$\Gamma = (\eta - \frac{\beta^2}{\eta} - \delta\beta^2)^{-\frac{1}{2}} \qquad \text{(II.17)}$$

For transverse Alfvénic perturbations the density and field strength perturbations are zero to first order. The conservation of mass [equation (II.11)] implies that

$$\frac{d}{dr}\ (r^2 \rho^* \Gamma\beta) = 0 \qquad \text{(II.18)}$$

If H_r is the covariant component of the time-independent

radial field, then one of the two non-trivial relations contained in equation (II.6a) is

$$\frac{d}{dr}\,(r^2 H_r) = 0 \tag{II.19}$$

By assumption, the transverse contravariant component H^θ is zero. If we take

$$H^\phi = \frac{\delta H}{r \sin\theta}$$

then equation (II.13) implies that

$$\begin{aligned} E^r &= E^\phi = 0 \\ E^\theta &= \frac{\delta E}{r} \end{aligned} \tag{II.20}$$

where

$$\delta E = \frac{\beta \delta H}{\eta} - \delta\beta\, H_r \tag{II.21}$$

From the second non-trivial relation in (II.6a) we have

$$\frac{1}{c}\frac{\partial}{\partial t}\,\delta H = -\frac{\eta}{r}\frac{\partial}{\partial r}\,(r\delta E) \tag{II.22}$$

The θ-component of the space part of the equation of motion [equation (II.10)] is

$$\cot\theta\left[\frac{\delta H^2 - \delta E^2}{4\pi\eta} - (\varepsilon + p)\,\Gamma^2\delta\beta^2\right] = 0 \tag{II.23}$$

and the ϕ-component of the same equation is

$$\begin{aligned} &(\varepsilon + p)\left[\Gamma^2\,\frac{1}{c}\frac{\partial}{\partial t}\,\delta\beta + \frac{\beta\Gamma}{r}\frac{\partial}{\partial r}\,(r\Gamma\delta\beta)\right] + \Gamma^2\beta\,\delta\beta\,\frac{\partial p}{\partial r} \\ &\quad = \frac{H_r}{4\pi}\left[\frac{1}{c\eta}\frac{\partial}{\partial t}\,\delta E + \frac{1}{r}\frac{\partial}{\partial r}\,(r\delta H)\right] \end{aligned} \tag{II.24}$$

Equations (II.22) and (II.24) can be solved for the WKB amplitudes under the assumptions that: 1) the wavelengths are small compared to local scale heights; 2) $\delta\beta$ and β_s are small compared to one, so that we can ignore second order terms in $\delta\beta$ and β_s. We do not assume that β_e or β are small compared to one. Since the solution to these equations is tedious we refer the interested reader to Appendix A, and merely quote the result. With the above assumptions, our solutions for the fluctuating quantities take the form

$$\begin{aligned} \delta\beta(r,t) &= \delta\beta(r)\ \exp\ [i(\omega t - S(r))] \\ \delta H(r,t) &= \delta H(r)\ \exp\ [i(\omega t - S(r))] \\ \delta E(r,t) &= \delta E(r)\ \exp\ [i(\omega t - S(r))] \end{aligned} \qquad \text{(II.25)}$$

where ω is angular frequency and dS/dr is the wave number of the wave. For notational convenience, we shall not distinguish between the full, rapidly varying functions of space and time, such as $\delta\beta(r,t)$, and their WKB amplitudes, such as $\delta\beta(r)$, which are slowly varying functions of space alone. If the meaning is not clear from context, we explicitly note the appropriate functional dependence on space and time. We define the velocity $c\beta_a$ as

$$\beta_a = \left[1 + \frac{4\pi\rho^* c^2}{H_r^{\,2}}\right]^{-\frac{1}{2}} \qquad \text{(II.26)}$$

In the limit that β_e is zero, $c\beta_a$ is simply the local Alfvén velocity (see, for example, Harris 1957). If we let $k = dS/dr$, then $c\beta_p$, the phase velocity of the waves, is given by ω/k.

For outwardly propagating waves, we then find

$$\beta_p = \frac{\beta + \eta\beta_a}{1 + \beta\beta_a/\eta} \tag{II.27}$$

In the limit that β_e is zero ($\eta = 1$), the phase velocity $c\beta_p$ is the proper relativistic sum of the streaming velocity $c\beta$ and the local Alfvén velocity $c\beta_a$. In the absence of streaming and in the limit that ρ^* goes to zero, the phase velocity of the waves becomes equal to the local speed of light, ηc. Note that since β cannot exceed η [cf. equation (II.17)] and β_a cannot exceed one, the phase velocity of the waves cannot in any circumstance exceed the local speed of light. The amplitudes $\delta H(r)$, $\delta E(r)$, and $\delta\beta(r)$ are simply related by

$$\delta H = \frac{\eta\ \delta E}{\beta_p}$$
$$\delta\beta = -\frac{\delta E(1 - \beta/\beta_p)}{H_r} \tag{II.28}$$

We may verify that the θ-component of the momentum equation [equation (II.23)] is identically zero for δE, δH, and δB related in this way. The WKB solution for $\delta E(r)$ is [see (A.16) in App. A]

$$\frac{r^2\delta E^2}{\beta_a} = \text{const} \tag{II.29}$$

The corresponding expressions for the radial dependence of δH and $\delta\beta$ can be obtained from equation (II.28). In particular, we find from equations (II.28) and (II.29) that

$$\delta\beta^2 = \text{const}\ \frac{\beta_a^{\,3}\ r^2}{\Gamma^4(\beta + \eta\beta_a)^2} \tag{II.30}$$

In deriving equation (II.30), we have approximated $1/\Gamma^2$ as $(\eta - \beta^2/\eta)$. This is valid in the present context, since we are writing an expression for a quantity already assumed to be small, and thus need not include corrections to that expression which are of order $\delta\beta^2$ as compared to the leading term. We cannot make this approximation unless our leading terms are already small. It is also convenient to express $\delta\beta^2$ in an equivalent form. We note that the definition of β_a [equation (II.26)] implies that

$$\frac{\beta_a^2}{1 - \beta_a^2} = \frac{H_r^2}{4\pi\rho^* c^2} \qquad \text{(II.31)}$$

Using the conservation of mass and magnetic flux, we obtain from equations (II.30) and (II.31) the form

$$\delta\beta^2 = \text{const}\ \frac{\beta\beta_a(1 - \beta_a^2)}{\Gamma^3(\beta + \eta\beta_a)^2} \qquad \text{(II.32)}$$

In the above discussion, the ϕ-polarization was chosen because Alfvénic perturbations in this direction can be simultaneously fitted together in a consistent manner over the surface of the entire sphere. This is not possible for waves polarized in the θ-direction (in particular, note the behavior at the poles of a spherical polar coordinate system). Locally, however, the solutions should be valid for arbitrary polarizations, and in particular in the equatorial plane of our coordinate system, both θ- and ϕ-polarizations obey the same equations. For convenience, in the in what follows we shall take

the waves as circularly polarized in the equatorial plane, with the WKB amplitudes for circular polarization in the same form as equations (II.28) through (II.32). The assumption of circular polarization has the advantage that for monochromatic waves, quantities such as $\delta\underset{\sim}{E}(r,t)\cdot\delta\underset{\sim}{E}(r,t)$, $\delta\underset{\sim}{E}(r,t)\times\delta\underset{\sim}{H}(r,t)$, etc., are no longer functions of time. In addition, field strength and density perturbations are zero to all orders, with the consequence that large-amplitude Alfvén wave solutions are possible (for example, see the treatment by Barnes and Suffolk 1971).

c) The Total Energy Flux

Having solved for the transverse wave amplitudes, we now seek an equation for the conservation of total energy flux in the radial direction, including energy flux due to the presence of Alfvén waves. We first note that the conserved mass flux F_M is given by

$$F_M = 4\pi r^2 \Gamma \rho^* c \beta \tag{II.33}$$

The time component of equation (II.9) is $T_o{}^{\mu}{}_{;\mu} = 0$. Using the expression for $T^{\mu\nu}$ given by equation (II.8), we have

$$\frac{d}{dr}\left\{4\pi r^2\left[(\varepsilon+p)\Gamma^2\beta c\eta + \frac{c}{4\pi}\,\delta E\,\delta H\right]\right\} = 0 \tag{II.34}$$

The second term inside the brackets is just the radial component of the Poynting vector. Using equations (II.16) and (II.33), we have that the total energy flux F_E is given by

$$F_E = c^2 F_M\left[\left(1 + \frac{\beta_s^2}{\alpha-1}\right)\Gamma\eta + \frac{\delta E\,\delta H}{4\pi c^2 \rho^* \Gamma \beta}\right] \tag{II.35}$$

This expression includes the energy flux due to the rest mass energy associated with the mass flux F_M. We consider the non-relativistic reduction of equation (II.35) in a subsequent paragraph.

For the moment, assume that we have wind solutions, and let $c\beta_\infty$ be the radial streaming velocity at infinity, with $\gamma_\infty = (1 - \beta_\infty^2)^{-\frac{1}{2}}$. Then for a given mass and total energy flux, we have

$$\gamma_\infty = \frac{F_E}{c^2 F_M} \tag{II.36}$$

The expression in brackets in equation (II.35) is F_E/c^2F_M and is also constant along a streamline. We shall find it convenient to write this expression in several ways. First, from equation (II.28), $\delta E\ \delta H = \eta \delta E^2/\beta_p$, with β_p given by equation (II.27), and from equation (II.29) we have

$$\delta E^2 = \frac{\delta E_o^{\,2} r_o^{\,2} \beta_a}{r^2 \beta_{ao}}$$

where the subscript "o" refers to some reference level r_o. The term in brackets in equation (II.35) becomes

$$(1 + \frac{\beta_s^{\,2}}{\alpha - 1})\Gamma\eta + \frac{\delta E_o^{\,2}}{\beta_{ao}(4\pi\rho_o{}^*\Gamma_o\beta_o c^2)} \frac{\beta_a(\eta + \beta\beta_a)}{\beta + \eta\beta_a} = \text{const} \tag{II.37}$$

We may also write this in terms of $\delta\beta^2$. Using equations (II.27) and (II.28), we have

$$\delta E\ \delta H = \Gamma^4\ \delta\beta^2\ H_r^{\,2}\ \frac{(\eta + \beta\beta_a)\ (\beta + \eta\beta_a)}{\beta_a^{\,2}} \tag{II.38}$$

From equations (II.31) and (II.38), we find that the term in brackets in equation (II.35) can be written as

$$(1 + \frac{\beta_s^2}{\alpha - 1})\Gamma\eta + \Gamma^3 \delta\beta^2 \frac{(\eta + \beta\beta_a)(\beta + \eta\beta_a)}{\beta(1 - \beta_a^2)} = \text{const} \qquad \text{(II.39)}$$

By simple algebraic manipulation, we can also write equation (II.39) as

$$(1 + \frac{\beta_s^2}{\alpha - 1})\Gamma\eta + \frac{\delta\beta^2\Gamma^3}{\beta\beta_a(1 - \beta_a^2)}(\beta + \eta\beta_a)^2 - \frac{\delta\beta^2\Gamma^3}{\beta_a}(\beta + \eta\beta_a) = \text{const} \qquad \text{(II.40)}$$

From equation (II.32) we see that the second term in this equation is constant, so that we have for any r the relation

$$(1 + \frac{\beta_s^2}{\alpha - 1})\Gamma\eta - \frac{\delta\beta^2\Gamma^3}{\beta_a}(\beta + \eta\beta_a) = \text{const} \qquad \text{(II.41)}$$

d) The Radial Equation of Motion

We have obtained an expression for the conserved energy flux in terms of background parameters alone, and thus have found implicitly all solutions $\beta(r)$ which satisfy that equation. To facilitate the imposition of critical point requirements, however, we need an explicit differential equation for the streaming velocity β. We may obtain such an equation by considering the radial component of equation (II.10). Since we have assumed purely radial expansion with

a polytrope relation between p and ρ^*, we may also obtain an equation for $d\beta/dr$ by differentiating any of the above expressions for the energy flux. We follow the latter course, using equation (II.37). The differentiation is a straightforward process, although tedious due to the fact that Γ is a complicated function of β and ρ^* [cf. equations (II.17), (II.26), and (II.30)]. First, we write equation (II.18) for the conservation of mass as

$$\frac{1}{\rho^*}\frac{d\rho^*}{dr} + \frac{1}{\Gamma}\frac{d\Gamma}{dr} + \frac{1}{\beta}\frac{d\beta}{dr} + \frac{2}{r} = 0 \qquad \text{(II.42)}$$

In differentiating equation (II.37), we encounter terms involving derivatives of ρ^*, and we systematically eliminate them in favor of derivatives of $d\beta/dr$ and $d\Gamma/dr$, using equation (II.42). For example, we can easily show from equations (II.19) and (II.26) that

$$\frac{d\beta_a}{dr} = -\frac{1}{2}\beta_a(1-\beta_a^2)\left(\frac{1}{\rho^*}\frac{d\rho^*}{dr} + \frac{4}{r}\right) \qquad \text{(II.43)}$$

which is simply rewritten as

$$\frac{d\beta_a}{dr} = \frac{1}{2}\beta_a(1-\beta_a^2)\left(\frac{1}{\beta}\frac{d\beta}{dr} + \frac{1}{\Gamma}\frac{d\Gamma}{dr} - \frac{2}{r}\right) \qquad \text{(II.44)}$$

Proceeding in this fashion, and using simple relationships such as $d\eta/dr = \beta_e^2/r$ [cf. equation (II.4)], we write the differential form of equation (II.37) as

$$\frac{d\Gamma}{dr}[\eta(1 + \frac{2 - \alpha}{\alpha - 1}\beta_s^2) + (\eta\beta_a^2 + 2\beta\beta_a + \eta)\Gamma^2\delta\beta^2/2]$$

$$= \frac{1}{\beta}\frac{d\beta}{dr}[\eta\Gamma\beta_s^2 - \Gamma^3\delta\beta^2(\eta\beta_a^2 + 2\beta\beta_a - \eta)/2] \qquad \text{(II.45)}$$

$$- \frac{1}{r}[\beta_e^2\Gamma(1 + \frac{\beta_s^2}{\alpha - 1}) - 2\eta\Gamma\beta_s^2 - \Gamma^3\delta\beta^2(\eta + 2\beta\beta_a + \eta\beta_a^2 - \beta_e^2)]$$

To obtain a differential equation for β alone, we differentiate equation (II.17) for Γ to obtain $d\Gamma/dr$ in terms of $d\beta/dr$. Using equation (II.30) for $\delta\beta^2$, we find after some effort that the differential form of equation (II.17) is

$$\frac{d\Gamma}{dr}\{1 + \frac{\Gamma^2\delta\beta^2}{4(\beta + \eta\beta_a)}[\beta(5 + 3\beta_a^2) + \eta\beta_a(7 + \beta_a^2)]\}$$

$$= \frac{1}{\beta}\frac{d\beta}{dr}\{\frac{\Gamma^3\beta^2}{\eta} + \frac{\Gamma^3\delta\beta^2}{4(\beta + \eta\beta_a)}[\eta\beta_a(1 - \beta_a^2) - \beta(1 + 3\beta_a^2)]\} \qquad \text{(II.46)}$$

$$- \frac{1}{r}\{\frac{\beta_e^2\Gamma^3}{2}(1 + \frac{\beta^2}{\eta^2}) + \frac{\Gamma^3\delta\beta^2}{2(\beta + \eta\beta_a)}[\beta(1 - 3\beta_a^2) + 2\beta_a\beta_e^2 - \eta\beta_a(1 + \beta_a^2)]\}$$

We now combine equations (II.45) and (II.46) to write an equation for $d\beta/dr$ alone in the form

$$\frac{r}{\beta}\frac{d\beta}{dr} = \frac{\mathcal{F}(r,\beta)}{\mathcal{G}(r,\beta)} \qquad \text{(II.47)}$$

e) The Non-relativistic Reduction of the Equations of Motion

To demonstrate the correspondence between equation (II.47) and the familiar equation of motion for polytrope winds, we consider this equation in the limit that β and β_e are small compared to one. We do not assume that β_a is small compared to one. Neglecting third order terms and higher in small quantities in equations (II.45) and (II.46) [e.g., $\beta\delta\beta^2$, $\beta_e{}^2\delta\beta^2$, etc.], we find that in this limit $d\beta/dr$ is given by

$$\frac{r}{\beta}\frac{d\beta}{dr} = \frac{\frac{1}{2}\beta_e{}^2 - 2\beta_s{}^2 - \frac{\delta\beta^2}{2(\beta+\beta_a)}(1+\beta_a{}^2)(\beta_a+3\beta)}{\beta_s{}^2 - \beta^2 + \frac{\delta\beta^2}{4(\beta+\beta_a)}(1-\beta_a{}^2)(\beta_a+3\beta)} \qquad \text{(II.48)}$$

We have kept terms of the form $\beta\,\delta\beta^2/(\beta+\beta_a)$ (which at first appear to be third order) in equation (II.48) because of the possibility that $\beta_a \ll \beta$. Equation (II.48) can also be derived by more familiar techniques. For the convenience of the reader who is not at ease with the mathematical formalism used above, we derive equation (II.48) in Appendix B using the standard MHD equations when not only $\delta\beta$ and β_s but also β and β_e are small compared to one, with β_a unrestricted. In the limit that β_a is small compared to one, equation (II.48) reduces to the equations of motion used by Alazraki and Couturier (1971) and Belcher (1971). If $\delta\beta$ is zero, we obtain the standard form for the equations of motion of polytrope stellar winds.

We also demonstrate the correspondence between our expression for the total energy flux F_E and its more familiar forms. As above, we expand F_E assuming that β and β_e are small compared to one, and neglect third order terms in small quantities. In this limit, from equations (II.35) and (II.39) we have

$$F_E = c^2 F_M + 4\pi r^2 \{ c\beta [\tfrac{1}{2} c^2 \rho (\beta^2 + \delta\beta^2) + \frac{\alpha}{\alpha - 1} p - \tfrac{1}{2} c^2 \rho \beta_e^2] + \rho c^3 \delta\beta^2 \frac{\beta + \beta_a}{1 - \beta_a^2} \} \tag{II.49}$$

In the limit that β_a is a small compared to one, this expression for F_E reduces to that given by Belcher (1971, equation 26b) except for the rest mass energy flux term, $c^2 F_M$. For future convenience, we rearrange terms in equation (II.49) to obtain the form

$$F_E = c^2 F_M + c^2 F_M [\tfrac{1}{2} \beta^2 - \tfrac{1}{2} \beta_e^2 \xi + \delta\beta^2 \frac{\beta_a + 2\beta(1 - \beta_a^2/2)}{\beta(1 - \beta_a^2)}] \tag{II.50}$$

where ξ is given by

$$\xi = 1 + \frac{\delta\beta^2}{\beta_e^2} - \frac{2}{\alpha - 1} \frac{\beta_s^2}{\beta_e^2} \tag{II.51}$$

Note that the expression in brackets in equation (II.50) is $\gamma_\infty - 1$ in the situation that β and β_e are small compared to one.

III. NUMERICAL SOLUTIONS TO THE WIND EQUATIONS

In the preceding section, we have set up and formally solved the equations of motion for the dynamic expansion of a stellar corona. We now consider solutions to these equations which satisfy given initial conditions at some reference level r_o close to a coronal base. In this section we sketch a general numerical algorithm for obtaining wind solutions for given initial values. We exhibit a limited number of these full numerical solutions, and note some of their characteristic features. In Section IV, this qualitative information will enable us to obtain approximate analytic solutions to the critical point equations over some ranges of initial values.

We choose a value for the polytrope index α, and specify at some reference level r_o the escape velocity $c\beta_{eo}$, the Alfvén velocity $c\beta_{ao}$, the sound velocity $c\beta_{so}$, and the velocity perturbation $c\delta\beta_o$. If we also choose a value for $c\beta_o$, the radial velocity at r_o, then this value of β_o along with the set of initial conditions in the combination $(\beta_{eo}, \beta_{ao}, \delta\beta_o{}^2/\beta_{eo}{}^2, \beta_{so}{}^2/\beta_{eo}{}^2)$ is sufficient to determine β as a function of r. This function is not necessarily a wind solution to equation (III.1), as we have imposed no critical point requirements. To determine $\beta(r)$, we first note that equation (II.39) for the conserved energy flux divided by the mass flux is

$$(1 + \frac{\beta_s{}^2}{\alpha - 1})\Gamma\eta + \delta\beta^2\Gamma^3 \frac{(\eta + \beta\beta_a)(\beta + \eta\beta_a)}{\beta(1 - \beta_a{}^2)}$$

$$= (1 + \frac{\beta_{so}{}^2}{\alpha - 1})\Gamma_o\eta_o + \delta\beta_o{}^2\Gamma_o{}^3 \frac{(\eta_o + \beta_o\beta_{ao})(\beta_o + \eta_o\beta_{ao})}{\beta_o(1 - \beta_{ao}{}^2)} \qquad \text{(III.1)}$$

where the subscript "o" refers to the reference level. All quantities on the right hand side of equation (III.1) can be computed using our initial parameter set and β_o. On the left hand side, for a given r, we easily compute the local escape velocity using equation (II.3) in the form $\beta_e^2 = \beta_{eo}^2/Z$, where we define Z as

$$Z = \frac{r}{r_o} \tag{III.2}$$

Of course, η at r is then $1 - \beta_e^2$. We now guess a value β for the radial velocity at r, and check to see if this value satisfies equation (III.1). This process is complicated by the fact that Γ at r depends on $\delta\beta^2$ at r, which in turn depends on Γ at r in a complex way [cf. equations (II.17) and (II.30)]. To obtain an initial estimate of Γ we approximate Γ at r by $(\eta - \beta^2/\eta)^{-\frac{1}{2}}$. Using the conservation of mass [equation (II.18)], we estimate ρ^*/ρ_o^* at r to be $\Gamma_o\beta_o/\Gamma\beta Z^2$. Given an estimate of ρ^*/ρ_o^* at r, we obtain an estimate of β_a at r using equation (II.26) in the form

$$\beta_a = \left[1 + \frac{1 - \beta_{ao}^2}{\beta_{ao}^2} \frac{\rho^*}{\rho_o^*} Z^4\right]^{-\frac{1}{2}} \tag{III.3}$$

We then compute a first estimate of $\delta\beta^2$ at r using equation (II.32). We now improve our estimate of Γ at r by using this estimate of $\delta\beta^2$ in equation (II.17). We then compute a new estimate for ρ^*/ρ_o^* using the conservation of mass, and a new estimate for β_a and $\delta\beta^2$ using equations (III.3) and (II.32).

This leads to a better estimate for Γ, and so on. This process is iterated until the n^{th} estimate of Γ differs from the $(n-1)^{th}$ estimate by less than one part in 10^{10}. The square of the sound velocity at r [cf. equation (II.15)] is then $\beta_s^2 = \beta_{so}^2(\rho^*/\rho_o^*)^{\alpha-1}$. Given our guess for β at r, we have thus computed values for η, $\delta\beta^2$, β_a, Γ, and β_s^2 at r. We now check our guess for β by using these quantities to determine if equation (III.1) is satisfied. If not, we keep guessing until we find a value of β that does satisfy equation (III.1). Thus, for a given β_o and our initial values, we can determine β as a function of r.

We find the wind solution (if it exists) by choosing β_o such that β as a function of r passes through the critical point of the differential equation (II.47). For a fixed initial value set and variable β_o, the critical point (r_c, β_c) is determined by the requirement that $\mathcal{F}(r_c, \beta_c, \beta_o)$ and $\mathcal{G}(r_c, \beta_c, \beta_o)$ simultaneously vanish (we have explicitly noted the dependence of $\mathcal{F}$ and $\mathcal{G}$ on β_o). In addition, (r_c, β_c) must also lie on the solution $\beta(r)$ which satisfies equation (III.1); this requirement imposes a third condition of the form $\mathcal{H}(r_c, \beta_c, \beta_o) = 0$. We thus have three transcendental equations which determine the three quantities r_c, β_c, and β_o, and thus the wind solution $\beta(r)$. We refer to the combination $(Z_c, \beta_c/\beta_{eo}, \beta_o/\beta_{eo})$, where $Z_c = r_c/r_o$, as the solution set for the initial value set $(\beta_{eo}, \beta_{ao}, \delta\beta_o^2/\beta_{eo}^2, \beta_{so}^2/\beta_{eo}^2)$. We

determine the solution set for a given initial value set in a manner similar to the procedure used to determine $\beta(r)$ from equation (III.1). That is, we guess a solution set $(z_c, \beta_c/\beta_{eo}, \beta_o/\beta_{eo})$ compute the quantities Γ_c, ρ_c^*/ρ_o^*, β_{ac}, β_{sc}, $\delta\beta_c$ and η_c exactly as described above (the subscript "c" refers to the critical point), and check our guess by seeing if $\mathcal{F}$, $\mathcal{U}$, and $\mathcal{W}$ simultaneously vanish. Thus, given our initial value set and the additional critical point requirement, we determine the solution set and the wind solution for β as a function of r. For $r_o < r < r_c$, we look for solutions to equation (III.1) in the range $\beta_o < \beta < \beta_c$, and for $r > r_c$, we look for solutions in the range $\beta > \beta_c$.

In practice, of course, the transcendental equations which determine a solution set for a given initial value set are involved, and it is impossible to guess a correct solution set for these equations a priori. Computationally, our procedure for finding solution sets always begins with a known solution for a given initial value set. To find a new solution set for a different initial value set, we slowly vary one of the initial values and numerically follow the solution set into new regions of solution space, starting from the known solution set. Since our known solution set originally began with the Parker solutions to the stellar wind equations, all of our numerical solutions are in a real sense analytic continuations of Parker solutions into new regions of initial value space.

Using this algorithm, we have computed full numerical solutions for a large range of initial values, and we display

some of these solutions to indicate their general characteristics. We take ξ_o to be the quantity ξ as defined in equation (II.51) evaluated at the reference level. We recall that for Parker polytrope winds to exist, we must satisfy the inequality $\frac{2}{\alpha-1} \beta_{so}^2/\beta_{eo}^2 > 1$. Since we are considering only conditions under which thermally driven winds do not exist, the quantity ξ_o is always positive. To minimize thermal effects, we take the polytrope index α to be 5/3, the adiabatic value. We plot our solution sets as functions of $\delta\beta_o^2/\beta_{eo}^2$, with the remaining initial values held fixed for a given curve. Figure 1 gives values of z_c, β_c/β_{eo}, and β_o/β_{eo} as functions of $\delta\beta_o^2/\beta_{eo}^2$ for a value of log β_{ao} fixed at - 4.0 ($c\beta_{ao}$ = 30.0 km/sec) and a value of log β_{eo} equal to - 2.7 ($c\beta_{eo}$ = 598.6 km/sec). The curves labeled A, B, and C are for values of log $(\beta_{so}^2/\beta_{eo}^2)$ equal to - 1.0, - 1.4, and - 3.0 (corresponding to sound velocities of 189.3 km/sec, 119.4 km/sec, and 18.9 km/sec, respectively). We can determine β_∞/β_{eo} as a function of $\delta\beta_o^2/\beta_{eo}^2$, and this is also plotted in Figure 1.

For these same initial values, we plot in Figure 2 the constants of motion F_M and $F_E - c^2F_M$, and the quantity $F_E/c^2F_M - 1$, which is $\gamma_\infty - 1$. In considering the scales for the mass and energy fluxes, we must remember that we have not yet completely specified conditions at the reference level. Up to this point, we have used the reference density and field only in the combination $4\pi\rho_o^*/H_{ro}^2$, and the reference level and stellar mass only in the combination M/r_o. These combinations are sufficient for the solution of the critical point equations, but to express

our mass and energy fluxes in grams/sec and ergs/sec, we must in addition specify M (or r_o) and ρ_o^* (or H_o). We choose to consider our remaining independent variables as the stellar mass M_o and the number density N_o (where N_o is the rest mass density divided by the proton rest mass). Once these variables are specified, we have that r_o in centimeters is given by $3 \times 10^5 M/\beta_{eo}^2$ if M is measured in solar masses, and H_o^2 in gauss squared is given by $0.019 N_o \beta_{ao}^2/(1 - \beta_{ao}^2)$ if N_o is measured in number per cubic centimeter. It is clear from equations (II.33) and (II.35) that both F_E and F_M are proportional to $M^2 N_o$. To obtain absolute units in Figure 2, we choose M to be one solar mass and N_o to be $10^6 cm^{-3}$. Mass and energy fluxes for other choices of M and N_o can be obtained by scaling according to $M^2 N_o$. For our present choices, with $\log \beta_{ao} = -4.0$ and $\log \beta_{eo} = -2.7$, we have $r_o = 7.5 \times 10^{10}$ cm and $H_o = 0.14$ gauss. For reference, we note that for the solar wind, mass and energy fluxes are on the order of 10^{12} grams/sec and 3×10^{27} ergs/sec, respectively.

There are characteristic features of the curves presented in Figures 1 and 2 that are common to all of the numerical solutions obtained. First, the curves are not too sensitive to the temperature parameter $\beta_{so}^2/\beta_{eo}^2$, particularly when this ratio is small compared to one. Note that for moderate wave amplitudes, the energy flux $F_E - c^2 F_M$ is essentially independent of temperature. Second, there is a broad range over which our solutions exhibit power law dependencies on the wave amplitude

$\delta\beta_o/\beta_{eo}$. In this range, β_c/β_{eo} and Z_c are essentially constant, F_M and β_o/β_{eo} go as $\delta\beta_o^4/\beta_{eo}^4$, $F_E - c^2F_M$ goes as $\delta\beta_o^2/\beta_{eo}^2$, and $\gamma_\infty - 1$ goes as $(\delta\beta_o^2/\beta_{eo}^2)^{-1}$. For future reference, we call this power law regime the intermediate wave amplitude range. As we move toward lower wave amplitudes, we eventually encounter an abrupt, low-amplitude cutoff in our dynamic solutions, at which β_o and the mass flux abruptly fall to zero and the energy flux is well behaved, so that $\gamma_\infty - 1$ goes to infinity. This abrupt cutoff occurs as $\delta\beta_o^2/\beta_{eo}^2$ approaches $4\beta_{ao}\xi_o^3/27$ from above (for the curves A, B, and C in Figure 1, the cutoff occurs at $\delta\beta_o^2/\beta_{eo}^2 = 5.1 \times 10^{-6}$, 1.31×10^{-5}, and 1.47×10^{-5}, respectively). For wave amplitudes below this cutoff, wind solutions do not exist, but static solutions are possible, as we shall see later on. As we move toward higher wave amplitudes, we encounter two different phenomena, depending on whether β_{ao} is substantially greater than or smaller than β_{eo}. In the case $\beta_{ao} > \beta_{eo}$ (not shown), the power law behavior of the intermediate range holds until $\delta\beta_o^2/\beta_{eo}^2$ becomes comparable to one, at which point β_o/β_{eo} and r_c/r_o approach one. If we move substantially beyond this limit, r_c becomes less than r_o and β_o exceeds β_{eo}. In the case $\beta_{ao} < \beta_{eo}$, the power law behavior holds until $\delta\beta_o^2/\beta_{eo}^2$ approaches β_{ao}/β_{eo}. As is evident from Figure 2, $F_E - c^2F_M$ no longer increases as $\delta\beta_o^2/\beta_{eo}^2$ beyond this point, and in fact begins to decrease, with r_c/r_o increasing. Thus, as $\delta\beta_o^2/\beta_{eo}^2$ becomes comparable to the smaller of 1 and β_{ao}/β_{eo}, our simple power law dependencies disappear, and we

refer to this regime as the strong wave amplitude region.

Having determined the value of β_o/β_{eo} for a given set of initial values, we can compute $\beta(r)$, $\rho^*(r)$, and so on, using the algorithm previously described. In Figure 3, we show typical wind profiles for solution points on curve A of β_o in Figure 1, as marked. The profiles 1 through 5 in Figure 3 are for $\beta_{so}^2/\beta_{eo}^2 = 0.1$ and $\log(\delta\beta_o^2/\beta_{eo}^2) = -1.8, -2.8, -3.8, -4.68,$ and -5.32, respectively (corresponding to $c\delta\beta_o = 75.4$, 23.8, 7.5, 2.7 and 1.3 km/sec, respectively). The last amplitude in this series is below the cutoff for dynamic solutions, and the corresponding profiles represent static solutions, as discussed in Section V. Figure 3a gives profiles of ρ^*/ρ_o^* and β/β_{eo} as functions of r/r_o, and Figure 3b shows β_a and $\delta\beta/\beta_a$ as functions of r/r_o. We note that $\delta H/H$ is equal to $-\delta\beta/\beta_a$ if $\beta \ll 1$, so that the profile of $\delta\beta/\beta_a$ is essentially also that of $\delta H/H$. Figure 3c gives the wave amplitude $\delta\beta$ divided by β_{eo} and the ratio of the transverse velocity to the radial velocity, $\delta\beta/\beta$. In Figure 3d we plot the Alfvénic Mach number β/β_a, and the total wave energy flux A, normalized to its value at r_o. The energy flux A includes all terms in the total energy flux which are proportional to the squares of wave amplitudes. The vertical line on each curve marks the location of the critical points.

Except for the strong wave amplitude case (curve 1), the radial profiles exhibit rapid decreases in density at a radial distance which in the absence of waves would be the top of a static atmosphere, with correspondingly rapid increases in β_a,

β, and $\delta\beta$. Beyond this point, the density begins to fall off as $1/r^2$, the velocity increases slowly, approaching the constant $c\beta_\infty$, and $\delta\beta$ and β_a eventually begin to decrease, approaching zero far from the star. For future reference, we point out some of the prominent characteristics of the profiles corresponding to the intermediate range of wave amplitudes (curves 2, 3, and 4). First, because of the rapid decrease in density, β_s at the critical point is small compared to β and $\delta\beta$ there, even if β_s were much greater than these quantities at the reference level. Second, from Figure 3d we see that β is much less than β_a both at the reference level and the critical point. Finally, and most importantly, we consistently find that $\delta\beta$ and β are approximately equal at the critical point, with a value close to the escape velocity there, regardless of their initial values at the reference level. Because of this property, the different profiles of $\delta\beta$ and β in Figures 3a and 3c are hard to separate; in general, the lower the values of $\delta\beta$ and β very close to the star, the higher their values very far from the star. From Figure 3d, we see that the transfer of wave energy flux to kinetic streaming energy flux takes place gradually, with no steep gradients, and with essentially all of the wave flux at r_o going to streaming energy far from the star.

As $\delta\beta_o^2/\beta_{eo}^2$ decreases toward the low amplitude cutoff, the density profiles become increasingly rarefied, with the Alfvén velocity at the critical point approaching c. Beyond the critical point, $\delta\beta$ and β_a require much greater distances

for significant decrease, and β approaches its limiting velocity much more slowly. As $\delta\beta_o^2/\beta_{eo}^2$ approaches the smaller of 1 and β_{ao}/β_{eo}, the density profiles fall off less rapidly, and the gradients in β and β_a are correspondingly diminished. Above this point, either β_o becomes comparable to β_{eo} (if $\beta_{ao} > \beta_{eo}$) or β_c becomes comparable to β_{ac} (if $\beta_{ao} < \beta_{eo}$).

IV. APPROXIMATE SOLUTIONS TO THE CRITICAL POINT EQUATIONS IN SPECIAL CASES

a) Basic Assumptions

With experience based on the full numerical solutions presented above, we seek approximate analytic expressions for our solutions (Z_c, β_c/β_{eo}, β_o/β_{eo}) over various range of initial conditions. At the outset, we limit ourselves here to cases for which $\beta_{eo} << 1$ and $\beta_{ao} << 1$. Additional limitations on the ranges of our initial values will appear as we proceed. To obtain analytic solutions, we make reasonable assumptions as to conditions at the critical level and reference level, and we list the assumptions below. After finding solutions, we a posteriori check the validity of these assumptions.

Assumption A: $\beta << \beta_a$ at the critical level and at the reference level.

With this assumption, β must be small compared to one at the critical point. Since we have already assumed that β_e is small compared to one, the non-relativistic equation of motion (II.48) is appropriate, and our critical point occurs when both the numerator and denominator of this equation are zero. Dropping terms such as $\delta\beta^2\beta/\beta_a$ (third order small by assumption), the critical point equations become

$$\frac{\beta_{ec}^2}{4} - \beta_{sc}^2 = \frac{\delta\beta_c^2}{4}(1 + \beta_{ac}^2) \qquad \text{(IV.1)}$$

and

$$\beta_c^2 - \beta_{sc}^2 = \frac{\delta\beta_c^2}{4}(1 - \beta_{ac}^2) \qquad \text{(IV.2)}$$

Note that we have not assumed β_{ac} to be small compared to one. We may combine equations (IV.1) and (IV.2) to obtain

$$\beta_c^2 = \frac{\beta_{ec}^2}{4}\,\frac{(1 - \beta_{ac}^2)}{(1 + \beta_{ac}^2)} + \frac{2\beta_{ac}^2}{1 + \beta_{ac}^2}\,\beta_{sc}^2 \qquad \text{(IV.3)}$$

For the integrated form of the equation of motion, we use equation (II.41). To second order in small quantities, we have

$$\beta_{ec}^2 + \delta\beta_c^2 - \beta_c^2 - \frac{2}{\alpha-1}\beta_{sc}^2 = \beta_{eo}^2 + \delta\beta_o^2 - \beta_o^2 - \frac{2}{\alpha-1}\beta_{so}^2 \qquad \text{(IV.4)}$$

To find $\delta\beta^2$ at the critical point, we use equation (II.30). Under our present assumptions, neglecting terms of order $\delta\beta_o^2\beta_o/\beta_{ao}$, etc., we obtain

$$\delta\beta_c^2 = \delta\beta_o^2\,\beta_{ac}\,\frac{Z_c^2}{\beta_{ao}} \qquad \text{(IV.5)}$$

Assumption B: $\beta_o^2 << [\beta_{eo}^2 + \delta\beta_o^2 - 2\beta_{so}^2/(\alpha - 1]$

With this assumption, we may drop β_o^2 on the right-hand side of equation (IV.4). We take ξ_o to be the quantity ξ as defined in equation (II.51), evaluated at the reference level. As we have noted previously, we only consider situations in which $\xi_o > 0$. Then equation (IV.4) becomes

$$\beta_{ec}^2 + \delta\beta_c^2 - \beta_c^2 - \frac{2}{\alpha - 1}\beta_{sc}^2 = \beta_{eo}^2 \xi_o \qquad \text{(IV.6)}$$

Assumption C: $\beta_s^2 << \beta^2$ at the critical point.

This condition is one of the novel properties of wave driven winds. In thermally driven winds, of course, β_s^2 is on the order of β^2 at the critical point. The dynamical rationale for this condition will become clear when we consider the transverse velocity $c\delta\beta$ at the critical point. With this assumption, we may drop the terms containing β_{sc}^2 from the right-hand side of equation (IV.3) and from the left-hand side of equations (IV.1) and (IV.6). As we shall see below, the only time this is not justified is when β_{ac} is extremely close to 1. Equation (IV.3) is thus taken to be

$$\beta_c^2 = \frac{\beta_{ec}^2}{4} \frac{(1 - \beta_{ac}^2)}{(1 + \beta_{ac}^2)} \qquad \text{(IV.7)}$$

Equation (IV.1) is

$$\delta\beta_c^2 = \frac{\beta_{ec}^2}{1 + \beta_{ac}^2} \qquad \text{(IV.8)}$$

and equation (IV.6) becomes

$$\beta_{ec}^2 + \delta\beta_c^2 - \beta_c^2 = \beta_{eo}^2 \xi_o \qquad \text{(IV.9)}$$

Using equations (IV.7) and (IV.8) in (IV.9), and remembering that $\beta_{ec}^2 = \beta_{eo}^2/Z_c$, we obtain an equation for Z_c as a function of β_{ac} and ξ_o

$$Z_c = \frac{7 + 5\beta_{ac}^2}{4(1 + \beta_{ac}^2)} \frac{1}{\xi_o} \tag{IV.10}$$

We now solve for β_{ac} in terms of the conditions at the reference level by equating the expression for $\delta\beta_c$ from equation (IV.5) with that in equation (IV.8). If we define the variable χ_o by

$$\chi_o = \frac{27}{4} \frac{1}{\beta_{ao}\xi_o^3} \frac{\delta\beta_o^2}{\beta_{eo}^2} \tag{IV.11}$$

where ξ_o is defined by equation (II.51), then the resulting equation may be written as

$$\chi_o \frac{4\beta_{ac}(7 + 5\beta_{ac}^2)^3}{(12)^3(1 + \beta_{ac}^2)^2} = 1 \tag{IV.12}$$

Equation (IV.12) determines β_{ac} as a function of the initial conditions. Given β_{ac}, we immediately have Z_c from equation (IV.10), and from (IV.7) we find that

$$\frac{\beta_c}{\beta_{eo}} = \frac{1}{2Z_c^{\frac{1}{2}}} \frac{(1 - \beta_{ac}^2)^{\frac{1}{2}}}{(1 + \beta_{ac}^2)^{\frac{1}{2}}} \tag{IV.13}$$

To complete our solution, we need an expression for β_o/β_{eo}. From the conservation of mass, we have

$$\frac{\beta_o}{\beta_{eo}} = \frac{\beta_c}{\beta_{eo}} \frac{\rho_c^*}{\rho_o^*} Z_c^2 \qquad \text{(IV.14)}$$

Using equation (III.3), we obtain ρ_c^*/ρ_o^* as a function of β_{ac} and Z_c, so that equation (IV.14) becomes

$$\frac{\beta_o}{\beta_{eo}} = \frac{(1 - \beta_{ac}^2)^{3/2}}{(1 + \beta_{ac}^2)^{1/2}} \frac{\beta_{ao}^2}{\beta_{ac}^2} \frac{1}{2Z_c^{5/2}} \qquad \text{(IV.15)}$$

At this point, we have completely solved the critical point equations under the limiting assumptions A, B, and C. Given the initial values (β_{eo}, β_{ao}, $\delta\beta_o^2/\beta_{eo}^2$, $\beta_{so}^2/\beta_{eo}^2$), we compute the parameter χ_o using the definitions in equations (II.51) and (IV.11). Given χ_o, we then find that value of β_{ac} between zero and one which satisfies equation (IV.12) [if it exists]. The solution for (Z_c, β_c/β_{eo}, β_o/β_{eo}) follows immediately from equations (IV.10), (IV.13), and (IV.15). To demonstrate the range over which these expressions are valid, we plot in Figure 1 the analytic solutions along with the full numerical solutions for β_o/β_{eo} and r_c/r_o as functions of $\delta\beta_o^2/\beta_{eo}^2$, with $\beta_{so}^2/\beta_{eo}^2 = .1$. The analytic results from the above equations are indicated by dots. Our approximate analytic results are indistinguishable from the numerical results at low and moderate wave amplitudes, but at high wave amplitudes there is considerable disagreement between the two. In the following sections, we consider these regimes in more detail, in particular the low-amplitude

cutoff in our expressions, and the differentiation between "moderate" and "high" wave amplitudes.

b) The Low-Amplitude Cutoff

We examine the regions in initial parameter space near the abrupt, low-amplitude cutoff in β_o and β_c when considered as functions of $\delta\beta_o^2/\beta_{eo}^2$ (e.g., the left-most segments of the curves in Figure 1 and 2). From equations (IV.7) and (IV.15), it is obvious that these cutoffs occur as β_{ac} approaches one (or, equivalently, as ρ_c^* approaches zero). From equation (IV.12), β_{ac} becomes one when χ_o is one. If we take $1 - \beta_{ac}^2$ to be small and expand equation (IV.12) to first order in this small quantity, we obtain

$$1 - \beta_{ac}^2 = \frac{4}{3}(\chi_o - 1) \qquad \text{(IV.16)}$$

Using this form in equations (IV.10), (IV.13), and (IV.15), we have

$$z_c = \frac{3}{2\xi_o}$$

$$\frac{\beta_c}{\beta_{eo}} = \left[\frac{\xi_o}{9}(\chi_o - 1)\right]^{1/2} \qquad \text{(IV.17)}$$

$$\frac{\beta_o}{\beta_{eo}} = \beta_{ao}^2 \left(\frac{2}{3}\right)^4 \xi_o^{5/2} (\chi_o - 1)^{3/2}$$

As we show below, these solutions are valid in the ranges of initial parameters satisfying

$$\xi_o^5 \left(\frac{\beta_{so}}{\beta_{eo}}\right)^6 \beta_{ao}^4 \frac{2^{12}}{3^4} \ll \chi_o - 1 \ll 1 \qquad \text{(IV.18)}$$

To find the constants of motion for these solutions, we evaluate the expressions for F_M and F_E [equations (II.33) and (II.35)] at the reference level. Since β_o and β_{eo} are much less than one at r_o, we use the non-relativistic form for F_E given in equation (II.50). If we insert the solutions (IV.17) into (II.50), we find that the third term in (II.50) is much larger than the first two. The energy flux F_E is to an excellent approximation given by

$$F_E = c^2 F_M + 4\pi r_o^2 c^3 \beta_{ao} \, \delta\beta_o^2 \rho_o^* \qquad \text{(IV.19)}$$

The second term in equation (IV.19) is just the radial component of the Poynting flux associated with the Alfvén waves at r_o. Note that all of the wave energy flux at r_o appears at infinity in the form of streaming energy flux. The mass flux is simply $4\pi r_o^2 \rho_o^* c\beta_o$, with β_o given by equation (IV.17). The quantity $\gamma_\infty - 1$ is given by the third term inside the brackets in equation (II.50), and since $\beta_o \ll \beta_{ao}$, we have

$$\gamma_\infty - 1 = \delta\beta_o^2 \, \frac{\beta_{ao}}{\beta_o} \qquad \text{(IV.20)}$$

Evaluating this expression for the solutions given by equation (IV.17), and remembering that these expressions are valid only when χ_o is very close to one, we have to a good approximation

$$\gamma_\infty - 1 \simeq \frac{3}{4} \beta_{eo} \xi_o^{1/2} (\chi_o - 1)^{-3/2} \qquad \text{(IV.21)}$$

The restrictions on the range of applicability for the solutions in equations (IV. 17) arise from the requirement that our solutions must satisfy a posteriori the assumptions A, B, and C under which they were derived. The requirement that $|\chi_o - 1| << 1$ easily satisfies both A and B. Assumption C is more difficult to satisfy, for the following reason. Using (III.3) and assuming (IV.16) and (IV.17) to be valid, we find that the density at the critical point is

$$\frac{\rho_c^*}{\rho_o^*} = 2(\chi_o - 1)\ \beta_{ao}^2 \left(\frac{2}{3}\right)^5 \xi_o^4 \qquad \text{(IV.22)}$$

Since $\beta_{sc}^2 = \beta_{so}^2 (\rho_c^*/\rho_o^*)^{\alpha-1}$, we see that β_{sc}^2 goes to zero as $(\chi_o - 1)^{\alpha-1}$ as χ_o approaches one. However, if α is less than 2, according to equation (IV.17), β_c^2 goes to zero faster than this, as $(\chi_o - 1)$. As a consequence, even though β_{sc}^2 is usually much smaller than β_c^2, in the limit of extremely low density ρ_c^* (χ_o extremely close to one), β_{sc}^2 becomes comparable to β_c^2. Taking α to be 5/3, we can derive the lower limit in inequality (IV.18) from equations (IV.17) and (IV.22), and the requirement that $(\chi_o - 1)$ be large enough to insure that $\beta_{sc}^2 << \beta_c^2$. For all cases considered here, the lower limit given by inequality (IV.18) is extremely small, so that χ_o must be very close to unity before assumption C is violated. For example, none of our numerical solutions near cutoff even approach the lower limit in inequality (IV.18), so that the region below this limit and above $\chi_o = 1$ is very narrow.

For completeness, however, we give (but do not derive) the solutions appropriate to the situation when the lower limit in inequality (IV.18) is badly violated (e.g., $\beta_{sc}^2 >> \beta_c^2$). In this circumstance, we assume that β_{ac} is so close to one that the second term on the right hand side of equation (IV.3) dominates our expression for β_c^2. In this approximation, if we keep terms in equation (IV.6) only to order $(1-\beta_{ac}^2)^{2/3}$ (in particular, neglecting $(1-\beta_{ac}^2)$ as compared to $(1-\beta_{ac}^2)^{2/3}$), we find that

$$Z_c = \frac{3}{2\xi_o}$$

$$\frac{\beta_c}{\beta_{eo}} = \left[\frac{\xi_o}{12} (\chi_o - 1) \right]^{1/2} \qquad \text{(IV.23)}$$

$$\frac{\beta_o}{\beta_{eo}} = \frac{\beta_{eo}^3}{\beta_{so}^3} \frac{1}{2^6} (\chi_o - 1)^2$$

This solution is valid in the limited region of initial parameter space defined by

$$0 < \chi_o - 1 << \xi_o^5 \left(\frac{\beta_{so}}{\beta_{eo}}\right)^6 \beta_{ao}^4 \frac{2^7}{3^{5/2}} \qquad \text{(IV.24)}$$

The upper limit in inequality (IV.24) derives from the requirement that the second term on the right hand side of equation (IV. 3) be much larger than the first. The expression for F_E in this range is still given by equation (IV.19). The mass flux is proportional to β_o, as before, and $\gamma_\infty - 1$ is

$$\gamma_\infty - 1 = \frac{\xi_o^{\,3}\beta_{ao}^{\,2}\beta_{so}^{\,3}}{27\ \beta_{eo}^{\,2}} \quad \frac{2^8}{(\chi_o-1)^2} \tag{IV.25}$$

In deriving the lower limit in expression (IV.18) and the equations (IV.23), (IV.24), and (IV.25), we have for convenience assumed $\alpha = 5/3$. All other equations in this paper are for arbitrary values of α.

The above expressions [equation (IV.17) in the range (IV.18), and equation (IV.23) in the range (IV.24)] exhibit all of the cutoff properties of the numerical solutions in Figures 1 and 2. The mass flux goes to zero as $\chi_o \to 1$, $\gamma_\infty - 1$ goes to infinity as $\chi_o \to 1$, and the energy flux is well-behaved and approaches a well defined limit at cutoff. If we take $\chi_o = 1$, we see from equation (IV.19) that the minimum energy flux we can get from the system in the form of a wind is

$$F_E^{\min} = \frac{8}{27}\ \beta_{eo}\xi_o^{\,3}\left[\ 4\pi r_o^{\,2} c\beta_{eo}\ \frac{H_o^{\,2}}{8\pi}\ \right] \tag{IV.26}$$

The term in brackets is the energy flux that would arise if the reference magnetic field energy density were convected at the escape velocity $c\beta_{eo}$. We let W_o denote this energy flux:

$$W_o = 4\pi r_o^{\,2} c\beta_{eo}\ \frac{H_o^{\,2}}{8\pi} \tag{IV.27}$$

c) The Intermediate Amplitude Case

We now consider regimes where our initial wave amplitudes are well above the cutoff point, e.g., when the parameter χ_o defined in equation (IV.11) is well above one. In this regime, β_{ac} as given by equation (IV.12) is small compared to one, and we have

$$\beta_{ac} = \left(\frac{6}{7}\right)^3 \frac{2}{\chi_o} \qquad \text{(IV.28)}$$

Equations (IV.10), (IV.13), and (IV.15) then give

$$Z_c = \frac{7}{4\xi_o}$$

$$\frac{\beta_c}{\beta_{eo}} = \frac{\xi_o^{1/2}}{7^{11/2}} \qquad \text{(IV.29)}$$

$$\frac{\beta_o}{\beta_{eo}} = \frac{1}{2}\left(\frac{27}{8}\right)^2 \left(\frac{7}{6}\right)^6 \left(\frac{4}{7}\right)^{5/2} \xi_o^{-7/2} \frac{\delta\beta_o^4}{\beta_{eo}^4}$$

The numerical factor in the expression for β_o/β_{eo} is approximately 3.55. These expressions are valid in the regions defined by

$$\frac{4}{27}\beta_{ao}\xi_o^3 < \frac{\delta\beta_o^2}{\beta_{eo}^2} < \text{MIN}\left(1, \frac{\beta_{ao}}{\beta_{eo}}\right) \qquad \text{(IV.30)}$$

The symbol MIN(a,b) denotes the smaller of the quantities a and b. The lower limit here insures that we are well away from cutoff, with $\chi_o >> 1$ and $\beta_{ac} << 1$. The upper limits stem from assumption A ($\beta_c << \beta_{ac}$) and from assumption B

($\beta_o << \beta_{eo}$). Assumption C is easily satisfied, and in particular

$$\frac{\beta_{sc}^2}{\beta_c^2} = 14.8 \; \xi_o^{-7/3} \; \frac{\beta_{so}^2}{\beta_{eo}^2} \; \left(\frac{\delta\beta_o}{\beta_{eo}}\right)^{8/3} \qquad \text{(IV.31)}$$

We point out that if $\delta\beta_o/\beta_{ao} << 1$ and $\delta\beta_o/\beta_{eo} << 1$, then the upper limit in inequality (IV.30) is automatically satisfied.

We again evaluate the constants of motion at the reference level. Within the range defined by expression (IV.30), the third term is equation (II.50) for F_E at r_o is again much larger than the first two. For the intermediate case, our expression for F_E is simply the sum of c^2F_M and the wave energy flux at r_o [cf. equation (IV.19)]. Again we note that all of the wave energy flux at r_o appears at infinity in the form of streaming energy flux. The mass flux F_M is $4\pi r_o^2 \rho_o^* c\beta_o$, as before, and

$$\gamma_\infty - 1 = 0.28 \; \frac{\beta_{eo}^3}{\delta\beta_o^2} \; \beta_{ao} \; \xi_o^{7/2} \qquad \text{(IV.32)}$$

To obtain some idea as to the allowed range of the constants of motion, we let $\delta\beta_o^2/\beta_{eo}^2$ vary between the limits imposed by inequality (IV.30). Within these limits, $F_E - c^2F_M$ varies over the range

$$\frac{8}{27} \; \xi_o^3 \beta_{eo} \; W_o < F_E - c^2F_M < 2W_o \; \text{MIN}\left(1, \; \frac{\beta_{eo}}{\beta_{ao}}\right) \qquad \text{(IV.33)}$$

and is proportional to $\delta\beta_o^2/\beta_{eo}^2$. The mass flux F_M varies between

$$0.16\ \xi_o^{5/2}\ \frac{W_o}{c^2} < F_M < \frac{7.1}{\beta_{eo}^2 \xi_o^{7/2}}\ \frac{W_o}{c^2}\ \mathrm{MIN}\left(1,\ \frac{\beta_{eo}^2}{\beta_{ao}^2}\right) \qquad \text{(IV.34)}$$

and is proportional to $\delta\beta_o^4/\beta_{eo}^4$. The term W_o/c^2 [cf. equation (IV.27)] in expression (IV.34) is the mass flux which would arise if the equivalent mass density $H_o^2/8\pi c^2$ were convected outward from r_o with velocity $c\beta_{eo}$. The quantity $\gamma_\infty - 1$ varies between the approximate limits

$$2.0\ \beta_{eo}\xi_o^{1/2} > \gamma_\infty - 1 > 0.28\beta_{eo}^2\xi_o^{7/2}\ \mathrm{MAX}\left(1,\ \frac{\beta_{ao}}{\beta_{eo}}\right) \qquad \text{(IV.35)}$$

The symbol MAX(a,b) denotes the larger of the quantities a and b. The upper limit here has been assumed to be much less than one, so that $\gamma_\infty - 1 \simeq \beta_\infty^2/2$. If V_∞ is $c\beta_\infty$ and V_{eo} is $c\beta_{eo}$, then inequality (IV.35) can be written as

$$2.0\ \xi_o^{1/4}\ \sqrt{cV_{eo}}\ > V_\infty > \xi_o^{7/4}\ V_{eo}\ \mathrm{MAX}\left(1,\ \sqrt{\frac{\beta_{ao}}{\beta_{eo}}}\right) \qquad \text{(IV.36)}$$

In the intermediate range of wave amplitudes, we thus expect to find streaming velocities at infinity in the range given by inequality (IV.36), with an inverse dependence on $\delta\beta_o/\beta_{eo}$. All of these functional dependencies on $\delta\beta_o/\beta_{eo}$ agree with the power law behavior we expect on the basis of the full numerical solutions for the intermediate range of wave amplitudes (Figures 1 and 2).

d) The Strong Amplitude Case

In the strong amplitude case, when our initial wave amplitudes are greater than the upper limit given by inequality (IV.30), we have not been able to derive explicit analytic expressions. In the case that $\beta_{ao} > \beta_{eo}$, we see from equation (IV.29) that β_o becomes comparable to β_{eo} as the wave amplitude approaches the upper end of the intermediate amplitude range. This is an unrealistic situation for a reference level near the coronal base. In the case that $\beta_{ao} < \beta_{eo}$, the wind becomes super-Alfvénic at the critical point as $\delta\beta_o^2/\beta_{eo}^2$ exceeds β_{ao}/β_{eo}. Assumption A above is no longer justified, and our intermediate range solutions are inappropriate. In the strong amplitude regime, we note that in the expression for the energy flux given by equation (II.50), we can no longer neglect the $- 1/2\ \beta_e^2\xi$ term, since even at the upper end of the intermediate amplitude range it is becoming comparable to the third term. The qualitative behavior to be expected would be a decrease in $F_E - c^2 F_M$ as $\delta\beta_o^2/\beta_{eo}^2$ increases beyond β_{ao}/β_{eo}, since we are now subtracting two terms of comparable magnitude, and indeed this is the behavior our numerical solutions for $\beta_{ao} << \beta_{eo}$ exhibit in the strong amplitude domain (cf. Figure 2). Other than qualitative statements, however, we must rely on our numerical solutions in this range of wave amplitudes.

e) The Alfvénic Critical Point

In the numeric and analytic solutions obtained above, the energy flux associated with the waves decreases as we move away from the coronal base, with a corresponding increase in the streaming energy flux associated with the wind (cf. Figure 3d). A physical scale of obvious importance in this process is the radial distance from the star at which a significant fraction of the initial wave energy has been transferred to streaming energy. It is easily shown that this distance scale is on the order of the Alfvénic critical distance r_a (by definition, r_a is that point at which the radial streaming velocity is equal to the local Alfvén velocity). For example, consider equation (II.37) for the conserved energy flux divided by the mass flux times c^2. The second term in this equation is the wave Poynting flux divided by the mass flux times c^2. As long as $\beta_o << \beta_{ao}$ (i.e., the streaming is sub-Alfvénic at r_o), this term will decrease by about a factor of 1/2 in going from r_o to r_a. Of course, there are other wave terms in equation (II.37) in addition to the Poynting flux term, but similar considerations apply as to the scale height over which these terms show significant decrease. We see from our numerical solutions (e.g., Figure 3d) that Z_a (i.e., r_a/r_o) increases as $\delta\beta_o/\beta_{eo}$ decreases. In the following paragraph, we derive approximate expressions for Z_a appropriate to the intermediate range of wave amplitudes. We have not been able to derive such expressions for the strong amplitude and cutoff regimes, but from our numerical solutions, it appears that Z_a is close to

one for strong wave amplitudes (if $\beta_{ao} < \beta_{eo}$), and approches infinity as $\delta\beta_o/\beta_{eo}$ approaches the low amplitude cutoff. This circumstance again casts doubt on the physical significance of solutions just above cutoff.

We now seek an approximate expression for Z_a in the intermediate range of initial wave amplitudes. We recall that in this range, β and β_a are always small compared to one, with $\beta_o << \beta_{eo}$. From equation (II.30), we thus have, for any Z,

$$\delta\beta^2 \simeq \delta\beta_o{}^2 \frac{\beta_a{}^3}{\beta_{ao}} \frac{Z^2}{(\beta + \beta_a)^2} \qquad \text{(IV.37)}$$

and from equation (III.3) and the conservation of mass

$$\beta_a = \frac{\beta_{ao}}{Z} \left(\frac{\beta}{\beta_o}\right)^{1/2} \qquad \text{(IV.38)}$$

We also have $\beta_o << \beta_{eo}$, so that equation (II.41) is, for any Z,

$$\beta_e{}^2 - \beta^2 - \delta\beta^2 - \frac{2}{\alpha - 1}\beta_s{}^2 + 2\delta\beta^2 \frac{(\beta + \beta_a)}{\beta_a}$$

$$= \beta_{eo}{}^2 \xi_o \qquad \text{(IV.39)}$$

We now evaluate equations (IV.37) through (IV.39) at Z_a. From equation (IV.38), we have that β_a at Z_a is given by

$$\beta_a = \frac{\beta_{ao}{}^2}{Z_a{}^2} \frac{1}{\beta_o} \qquad \text{(IV.40)}$$

Using this expression in (IV.37), we obtain for $\delta\beta^2$ at Z_a

$$\delta\beta^2 = \frac{\delta\beta_o^2}{4} \frac{\beta_{ao}}{\beta_o} \tag{IV.41}$$

From equation (IV.20), we see that $\delta\beta^2$ at Z_a is just $\beta_\infty^2/8$. Using these expressions in (IV.39) and neglecting the sound velocity $c\beta_s$, we obtain a fourth order equation for Z_a of the form

$$\frac{\beta_{eo}^2}{Z_a} - \frac{\beta_{ao}^4}{\beta_o^2} \frac{1}{Z_a^4} + \frac{3}{8}\beta_\infty^2 = \beta_{eo}^2\xi_o \tag{IV.42}$$

For a rough estimate of Z_a, we note that expression (IV.36) indicates that β_∞^2 is significantly greater than β_{eo}^2 except at the upper end of the intermediate amplitude range. If we neglect terms involving β_{eo}^2 in equation (IV.42), we find that

$$Z_a^4 = \frac{\beta_{ao}^4}{\beta_o^2} \frac{8}{3\beta_\infty^2} \tag{IV.43}$$

From equation (IV.40) and (IV.43), we note that β^2 at Z_a is $3\beta_\infty^2/8$. Using equation (IV.29) for β_o and (IV.20) for β_∞, equation (IV.43) becomes

$$Z_a = 0.80\left(\frac{\beta_{ao}}{\beta_{eo}} \frac{\beta_{eo}^2}{\delta\beta_o^2}\right)^{3/4} \tag{IV.44}$$

Assuming that $\beta_{ao} < \beta_{eo}$, we find that in the intermediate range of wave amplitudes defined by expression (IV.30), Z_a varies

over the range

$$3.3\ \beta_{eo}^{-3/4}\ \xi_o^{-11/8} > Z_a \gtrsim 1 \qquad \text{(IV.45)}$$

The lower bound here is suspect, as it occurs at the upper end of the intermediate amplitude range, and in this region we are not justified in neglecting the β_{eo}^2 terms in equation (IV.42). As long as we stay away from the upper limit in inequality (IV.30), however, equation (IV.44) for Z_a is reasonably accurate, as may be verified by comparison with the full numerical results in Figure 3d.

V. STATIC ATMOSPHERES

We have found in previous sections that for initial wave amplitudes below a certain minimum value defined by inequality (IV.30), wind solutions to the equations of motion no longer exist. Since the mass flux of the dynamic solutions decreases to zero as the initial wave amplitude decreases toward the minimum value, it seems plausible to expect that below this minimum value only static atmospheres occur. This is indeed the case, as we shall demonstrate.

Even though the development in Section IIc above assumes throughout that a dynamic expansion exists, we may extract the equations appropriate to the static situation by taking the limit $\beta \to 0$. We do not use equation (II.39) for this purpose because of the singularity as $\beta \to 0$, but rather equation (II.41). In the limit that β is zero, we have

$$\frac{\left(1 + \frac{1}{\alpha-1}\beta_s^2\right)\left(1-\beta_e^2\right)}{\sqrt{1 - \beta_e^2 - \delta\beta^2}} - \delta\beta^2\Gamma^3\eta = \text{const.} \qquad \text{(V.1)}$$

For simplicity we assume that $\beta_e^2 << 1$, so that this equation to second order is

$$1 + \frac{1}{\alpha-1}\beta_s^2 - \frac{1}{2}\beta_e^2 - \frac{1}{2}\delta\beta^2 = 1 + \frac{1}{\alpha-1}\beta_{so}^2 - \frac{1}{2}\beta_{eo}^2 - \frac{1}{2}\delta\beta_o^2 \qquad \text{(V.2)}$$

From equation (II.30), $\delta\beta^2$ in the limit $\beta \to 0$ is

$$\delta\beta^2 = \delta\beta_o{}^2 \frac{\beta_a}{\beta_{ao}} Z^2 \tag{V.3}$$

where $Z = r/r_o$. From equation (III.3) for ρ^*/ρ_o^*, we see that β_a can be expressed as a function of Z and ρ^*/ρ_o. Of course the sound velocity is $\beta_s{}^2 = \beta_{so}{}^2 (\rho^*/\rho_o^*)^{\alpha-1}$. With these expressions, we can write equation (V.2) in terms of ρ^* and Z alone

$$\frac{\beta_{eo}{}^2}{Z} - \frac{2}{\alpha-1} \beta_{so}{}^2 \left(\frac{\rho^*}{\rho_o^*}\right)^{\alpha-1} + \frac{\delta\beta_o{}^2}{\beta_{ao}} \frac{Z^2}{\left[1 - \frac{1-\beta_{ao}{}^2}{\beta_{ao}{}^2} \frac{\rho^*}{\rho_o^*} Z^4\right]^{1/2}}$$

$$= \beta_{eo}{}^2 \xi_o \tag{V.4}$$

where ξ_o is given by equation (II.51). Equation (V.4) defines ρ^*/ρ_o^* as a function of Z.

If a static atmosphere is to exist, we expect a top to that atmosphere and we now consider whether there exists a Z_τ such that $\rho^*(Z_\tau) = 0$. If such a point exists, we see from equation (III.3) and (V.4) that it must satisfy the equation

$$\frac{\beta_{eo}{}^2}{Z_\tau} + \frac{\delta\beta_o{}^2}{\beta_{ao}} Z_\tau{}^2 = \beta_{eo}{}^2 \xi_o \tag{V.5}$$

This cubic equation for Z_τ does not have a real root greater than one if $\xi_o < 1$. This is the regime of the thermally driven wind solutions. If $\xi_o > 0$ and $\chi_o > 1$ [cf. equation (IV.11)], there are also no real roots greater than one. This is the regime of the wave-driven winds, as in Section IV. However, if $\xi_o > 0$ and $\chi_o \leq 1$, there exists a real root greater than one, and therefore a top to a static atmosphere. If we define the angle ϕ such that

$$90° \leq \phi < 180°$$
$$\cos \phi = - \chi_o^{1/2} \tag{V.6}$$

then the top of the atmosphere occurs at

$$Z_\tau = \frac{3}{\xi_o \chi_o^{1/2}} \cos \left(\frac{\phi}{3} + 240°\right) \tag{V.7}$$

In the limit that $\delta\beta_o$ goes to zero, χ_o goes to zero, and $\phi \to 90° + \chi_o^{1/2}$, so that Z_τ is approximately $[1-2\beta_{so}^2/\beta_{eo}^2(\alpha-1)]^{-1}$. This is the usual expression for the top of a gravitationally contained polytrope atmosphere.

Thus, if the initial wave amplitudes are below the limit given by $\chi_o = 1$, our atmosphere is static, with a density profile given by equation (V.4) and a top Z_τ given by equation (V.7). The static density profile plotted in Figure 2 is computed on the basis of these equations. In these configurations, the static atmosphere is modified by the presence of the waves,

but the waves propagate outward from r_o with no decrease in energy flux. They emerge from the top of the atmosphere traveling at the speed of light in vacuum, with δE^2 and δH^2 subsequently decreasing as $1/r^2$ [cf. equation (II.29)].

VI. LIMITATIONS OF THE MODEL

Under various restrictive assumptions, we have formulated and found solutions to a well-defined mathematical model of a physical situation. Before summarizing the properties of these solutions, we point out their probable defects and the pitfalls involved in applying them to real astrophysical situations. First, the assumption of radial fields is a strong one, particularly in the circumstance that field pressures are large compared to kinetic pressures, and closed field configurations are to be expected. In such cases, qualitative properties of our model will apply only in regions where the field lines are close to radial for various reasons (most obviously, in the polar regions of a magnetic dipole). We note that the crucial feature which gives rise to the possibility of wave driven winds is the rapid fall-off with radial distance of the density as compared to the field strength, and the consequent rapid increase of $c\delta\beta$, the transverse perturbation velocity, with radius. This situation will obtain as long as H falls off inversely as a low power of r, and it may not be unreasonable to expect wave-driven expansion in the polar regions of a strong magnetic dipole. Short of a detailed calculation, however, we can only speculate.

For the MHD approximation to be valid, we must have wave frequencies which are small compared to cyclotron frequencies and densities which are high enough to make the concept of a fluid meaningful. For the latter reason, the dynamic solutions just above cutoff, for which the mass flux approaches zero (Section IVb), and the static solutions below cutoff, in which

the density goes to zero at the atmospheric top (Section V), should be viewed with caution. In addition to this upper limit on the frequency ω, we must also satisfy a lower bound of the form $\omega >> \delta V/r$ for all r, otherwise the transverse particle displacement associated with the wave will be an appreciable fraction of $2\pi r$. Since $\delta V(r)$ increases much more rapidly than r, reaching the local escape velocity within a few stellar radii, this lower bound is not inconsequential, especially for small objects with high escape velocities.

We have ignored any possibility of wave damping, even though we may have a situation where the velocity perturbation $c\delta\beta$ increases dramatically with radius, approaching the escape velocity in a distance on the order of a stellar radius. However, we note that β_a also increases rapidly outward,so that initially $\delta\beta/\beta_a$ actually decreases with increasing radius, as does $\delta H/H$ (see Figure 3). In addition, there are reasons to believe that circularly polarized Alfvén waves in a completely ionized, rarefied plasma are difficult to damp both from an observational and theoretical standpoint (Belcher and Davis, 1971; Barnes, 1966).

Finally, in retrospect, one of the strongest assumptions we have made is that wavelengths are short compared to local scale heights. In many of our numerical solutions (cf. Figure 3), there are regions near the top of otherwise static atmospheres in which wave amplitudes and radial velocities exhibit spectacular increases over short distances and the short wavelength approximation here becomes suspect, at the least. The situation

improves somewhat if we depart from an adiabatic atmosphere ($\alpha \neq 5/3$), as this tends to smooth out the abrupt gradients, and the proper inclusion of non-WKB terms would probably have the same effect. It is not clear how the inclusion of such terms would change the dynamical situation (energy and mass fluxes, etc.), although we would hope for no qualitative changes. To answer the question properly requires the numerical integration of the full transverse equations of motion, in conjunction with the radial momentum equation.

VII. SUMMARY

We have investigated the properties of stellar winds in which the only source of energy flux is due to low frequency, undamped Alfvén waves propagating outward along radial magnetic field lines. The thermal properties of the plasma are described by a polytrope relation, and we have considered only situations which would lead to static atmospheres in the absence of waves. We have demonstrated that Alfvén waves of sufficiently large amplitude are capable of driving the supersonic, super-Alfvénic expansion of the plasma, with a complete transfer of wave energy flux near the star to streaming energy flux far from the star.

The process responsible for the acceleration of such winds is intrinsically different from that which produces thermally driven winds. To illustrate these differences, we discuss briefly the features of the non-relativistic solutions. Let us denote $c\beta$ by V, $c\delta\beta$ by δV, $c\beta_a$ by V_a, $c\beta_s$ by V_s, and $c\beta_e$ by V_e. In the situation that V is much less than V_a, which is in turn much less than c, the differential equation for the radial velocity V is (cf. equation II.48)

$$\frac{r}{V}\frac{dV}{dr} = \frac{1}{2}\frac{V_e^2 - 4(V_s^2 + \delta V^2/4)}{(V_s^2 + \delta V^2/4) - V^2} \qquad \text{(VII.1)}$$

In the absence of waves, this equation reduces to the familiar polytrope form for the radial gradient of V. In the presence of waves, the velocity perturbation δV complements the local sound velocity V_s. The dynamical effects of these two velocity

terms are drastically different, however, because of their differing behavior as a function of radial distance from the coronal base. If ρ is the mass density and α the polytrope index, then V_s^2 is proportional to $(\rho)^{\alpha-1}$. Thus V_s^2 is at best a constant ($\alpha = 1$) and at worst decreases rapidly with distance from the coronal base ($\alpha = 5/3$). On the other hand, close to the star the Alfvén wave amplitudes vary so as to approximately conserve the wave energy flux $4\pi r^2 V_a (\rho \delta V^2)$. As a consequence, δV^2 is proportional to $r^2 V_a$ close to the star (cf. equation (II.30) for $V << V_a$). Since the density may decrease outward as a high inverse power of r, with H falling off only as $1/r^2$, the Alfvén velocity V_a can increase substantially over its initial value at some reference level r_o. Physically, the Alfvén waves are propagating outward into an increasingly rarefied atmosphere, and to conserve energy flux δV^2 must initially increase outward, rather than decrease, as does V_s^2.

The relative importance of the δV^2 and V_s^2 velocity terms in equation (VII.1) has a major influence on the nature of the critical point solutions of this equation. In the absence of waves, Parker (1963) has shown that equation (VII.1) will have well-behaved wind solutions for initial values at the reference level r_o in the range

$$\frac{\alpha - 1}{2} < \frac{V_{so}^2}{V_{eo}^2} < \frac{1}{4} \qquad \text{(VII.2)}$$

The lower limit in this inequality represents the point below.

which critical point solutions to equation (VII.1) no longer exist (the gravitational field is too strong to allow expansion and the corona assumes a static configuration). The upper limit represents the point above which conditions at the coronal base are no longer realistic (e.g., the streaming velocity is already supersonic at r_o). Consider the situation in which the lower limit in inequality (VII.2) is violated. In the absence of waves there will be no critical point solutions to equation (VII.1) because V_s^2 is never comparable to V_e^2. With waves, however, there is still a possibility of a wind solution if δV^2 at the critical point is comparable to V_e^2 there. Let the subscript "c" indicate evaluation at the critical point r_c (if it exists). The above discussion of the radial dependence of δV^2 implies that for δV_c^2 to be comparable to V_{ec}^2, we must have $\delta V_o^2 (r_c/r_o)^2 (V_{ac}/V_{ao})$ comparable to $V_{eo}^2 (r_o/r_c)$. Critical point solutions of this nature do in fact exist, and usually occur within a few stellar radii. For a given δV_o, we require that the density at r_c be low enough (and thus the value of V_{ac}/V_{ao} high enough) so that δV_c is comparable to V_{ec}. As δV_o becomes smaller, the density profiles become more rarefied, so that δV still attains the escape velocity at r_c. However, this process cannot continue indefinitely, since the maximum value possible for δV_c^2 is on the order $\delta V_o^2 (c/V_{ao})$, corresponding to the limit that V_{ac} is close to the speed of light (and assuming that r_c is on the order of r_o). If $\delta V_o^2 (c/V_{ao})$ is substantially below V_{eo}^2, δV_c can not reach the escape velocity at r_c, and critical point solutions do not exist.

We note that Alazraki and Couturier (1971) and Belcher (1971) allow arbitrarily large Alfvén velocities when considering, the problem. In such a situation, δV_c can reach V_{ec} no matter how small δV_o, as long as it is non-zero. As a result, these authors incorrectly conclude that wind solutions are always possible if $\delta V_o^2 > 0$.

These heuristic arguments provide some qualitative insight into the range of initial wave amplitudes necessary for the production of Alfvén winds. If we assume that V_{eo} and V_{ao} are small compared to c, then our detailed mathematical treatment indicates that well-behaved wind solutions exist for initial wave amplitudes in the range

$$\frac{4}{27}\,\xi_o^{\,3}\,\frac{V_{ao}}{c} \;<\; \frac{\delta V_o^{\,2}}{V_{eo}^{\,2}} \;<\; \mathrm{MIN}\left(1,\ \frac{V_{ao}}{V_{eo}}\right) \qquad \text{(VII.3)}$$

where ξ_o is a factor of order unity for our purposes [cf. equation (II.51)]. We emphasize that inequality (VII.3) only applies when the lower limit in inequality (VII.2) is violated (e.g., when there are no Parker wind solutions). Under various assumptions, we have obtained approximate analytic solutions to the critical point equations for initial wave amplitudes in the range defined by inequality (VII.3). We have referred to this range (which does <u>not</u> include the lower limit) as the intermediate amplitude range. Initial wave amplitudes just above and inclusive of the lower limit of inequality (VII.3) are said to be in the cut-off regime, as discussed below. Initial wave amplitudes below this lower limit are too weak to drive the coronal expansion,

and the atmosphere assumes a gravitationally bound, static configuration. Wind solutions exist for initial wave amplitudes above the upper limit in inequality (VII.3) (referred to as the strong amplitude regime), but they are such that either $V_o \gtrsim V_{eo}$ (if $V_{ao} > V_{eo}$) or $V_c \gtrsim V_{ac}$ (if $V_{ao} < V_{eo}$). The situation in which $V_o \gtrsim V_{eo}$ is clearly unrealistic for a reference level at a coronal base. Although the situation in which $V_c \gtrsim V_{ac}$ at r_c does not necessarily imply that conditions at r_o are unrealistic, it does prevent us from obtaining approximate analytic solutions to the critical point solutions. We must rely on numerical solutions for wave amplitudes above this limit, and as a consequence our understanding of the properties of solutions in the strong amplitude regime is limited. For wave amplitudes in the intermediate and cutoff regimes, however, our understanding is detailed.

Before considering these properties, we note as an aside that our choice of parameters for the specification of the initial conditions at r_o is neither unique nor necessarily ideal. For example, since δV and V_a vary rapidly as functions of radius, it may be difficult in practice to choose values for them at a given point, since they are sensitive functions of distance from the star. A quantity which may be more appropriate as an initial value is the Alfvén wave Poynting flux at r_o, $4\pi r_o^2 (c\, \delta E_o\, \delta H_o/4\pi)$, since this flux is essentially constant close to the star. If we denote this flux by F_p^o, and let W_o be $4\pi r_o^2\, V_{eo}\, (H_o^2/8\pi)$, then over the range of wave

amplitudes in equation (VII.3), F_p^o varies between the limits

$$\frac{8}{27}\,\xi_o^3\,\frac{V_{eo}}{c}\,W_o \;<\; F_p^o \;<\; 2W_o\,\mathrm{MIN}\left(1,\,\frac{V_{eo}}{V_{ao}}\right) \qquad \text{(VII.4)}$$

Well-behaved wind solutions will exist if the Poynting flux associated with the Alfvén waves at r_o lies in the range given by expression (VII.4). This requirement on the Poynting flux for the existence of well-behaved wind solutions is completely equivalent to the requirement on the wave amplitudes given above.

The properties of stellar winds which are of primary interest are their energy fluxes, mass fluxes, and energies per particle at infinity. For initial wave amplitudes in the intermediate range, the streaming energy flux at infinity is equal to the Poynting energy flux at the reference level, F_p^o. In this range, the energy flux at infinity therefore varies between the limits of expression (VII.4) and is proportional to δV_o^2. The mass flux F_M in the intermediate range varies between the limits given in expression (IV.34) and is proportional to δV_o^4. The lower limit in this expression does not include the abrupt decrease in mass flux as δV_o^2 approaches cutoff. The limiting velocity V_∞ of the wind for the intermediate range varies between the limits given in inequality (IV.36) and is proportional to $1/\delta V_o$. Again, the upper limit in this equation does not include the violent behavior in the regime of wave amplitudes just above cutoff. The distance required for a significant transfer of the initial wave energy flux F_p^o

to wind streaming energy flux is of the order of r_a, where r_a is the point at which the radial streaming velocity is equal to the local Alfvén velocity (Section IVe). For the intermediate range of wave amplitudes, assuming $V_{ao} < V_{eo}$, r_a varies between the limits given in inequality (IV.45), and is proportional to $\delta V_o^{-3/2}$. In the intermediate range, 75% of the kinetic energy per particle at r_a is associated with the radial streaming velocity, and 25% is associated with the transverse velocity of the wave.

As δV_o closely approaches the lower limit in expression (VII.3), the mass flux F_M decreases abruptly toward zero, and since the energy flux remains well-behaved, the energy per particle at infinity increases abruptly toward infinity. In the same limit, the distance r_a goes to infinity. Qualitatively, this situation arises from the fact that just above cutoff the Alfvén waves are able to drive a vanishingly small mass flux off the star. At cutoff, we have a finite wave energy flux at r_o which is to be distributed at infinity among an infinitesimal number of particles. Below cutoff, dynamic expansion is no longer possible, and the atmosphere formally assumes a static configuration. In the static case, the energy flux associated with the waves is rigorously conserved, and appears at infinity in the form of waves. As pointed out above, the physical significance of the dynamic solutions just above cutoff, and the static solutions below cutoff, are questionable because of the extremely low densities involved.

For the purposes of numerical illustration, consider a star with $V_{so}^2/V_{eo}^2 = 0.1$, $\alpha = 5/3$, $r_o = 0.75 \times 10^{11}$ cm, $V_{eo} = 599$ km/sec, and $H_o = 0.5$ gauss. From expression (VII.4), the initial Alfvén wave Poynting flux needed for the production of an Alfvén wind lies between the limits 0.85×10^{24} ergs/sec and 0.84×10^{29} ergs/sec. If we take a density at r_o of 1×10^8 particles/cc, the Alfvén velocity V_{ao} is 109 km/sec, and the intermediate range of wave amplitudes varies between 2.3 km/sec and 256 km/sec. For wave amplitudes in this range, we obtain the same streaming energy fluxes at infinity as Poynting fluxes ar r_o, and mass fluxes between the limits 3.1×10^6 gms/sec and 2.9×10^{14} gms/sec. The streaming velocities at infinity lie between 24,500 km/sec and 300 km/sec.

In conclusion, we note several points in comparing Alfvén winds with thermally driven winds. To obtain winds in the thermal polytrope models, the sound velocity at the coronal base must be on the order of the escape velocity there, and the limiting velocity at infinity is of the same order. In Alfvén winds, the initial transverse velocity δV_o can be small compared to the escape velocity, by as much as a factor of order $\sqrt{V_{ao}/c}$, and the limiting velocity at infinity can be large compared to the escape velocity, by as much as a factor of order $\sqrt{c/V_{eo}}$. Even in tightly bound atmospheres with small initial wave amplitudes ($\delta V_o^2 << V_{so}^2 << V_{eo}^2$), rarefied, energetic wind solutions may exist. The existence of such winds even in these extreme situations is closely related to the collective nature of the acceleration process, in which the energy input required to

maintain the low velocity, transverse motions of a great many ionized particles at a coronal base is ultimately transferred to the high velocity, radial streaming of relatively few particles far from the star. As a result, wave driven winds can exist even in tightly bound situations, and may exhibit relatively high energies per particle at infinity. It is this qualitative concept of the acceleration mechanism that we wish to emphasize, rather than the quantitative details of the solutions we have presented.

Appendix A

We solve equations (II.22) and (II.24) for the WKB wave amplitudes under the assumptions: 1) the wavelengths are small compared to the local scale heights; 2) $\delta\beta$ and β_s are small compared to one, so that we may neglect second order and higher terms in $\delta\beta$ and β_s. With these assumptions, we can immediately drop the last term on the left hand side of equation (II.24), and replace Γ everywhere by γ, where

$$\gamma = (\eta - \frac{\beta^2}{\eta})^{-\frac{1}{2}} \tag{A.1}$$

Strictly speaking, to justify this approximation, we must require that $\delta\beta$ be small compared to $1/\gamma$ rather than 1, but for our purposes γ can be taken to be close to unity.

We may also replace $(\varepsilon + p)$ in equation (II.24) by $\rho^* c^2$, so that equation (II.24) becomes

$$\rho^* c^2 \left[\gamma^2 \frac{1}{c} \frac{\partial}{\partial t} \delta\beta + \frac{\beta\gamma}{r} \frac{\partial}{\partial r} (r\gamma\delta\beta)\right] - \frac{H_r}{4\pi} \left[\frac{1}{c\eta} \frac{\partial}{\partial t} \delta E + \frac{1}{r} \frac{\partial}{\partial r} (r\delta H)\right] = 0 \tag{A.2}$$

We eliminate $\delta\beta$ from this equation by using equation (II.21) in the form

$$\delta\beta = \frac{1}{H_r} \left[\frac{\beta\ \delta H}{\eta} - \delta E \right] \tag{A.3}$$

For convenience, we introduce a new variable δh defined by

$$\delta h = \frac{\delta H}{\eta} \tag{A.4}$$

Using equations (A.3) and (A.4) in (A.2), we obtain after some manipulation an equation for δh and δE alone, as follows

$$\left[\gamma^2 + \frac{H_r^2}{4\pi\rho^* c^2 \eta} \right] \frac{1}{c} \frac{\partial}{\partial t} \delta E + 2\gamma^2 \beta \frac{\partial}{\partial r} \delta E$$

$$+ \left[\frac{\eta H^2 r}{4\pi\rho^* c^2} - \beta^2 \gamma^2 \right] \frac{\partial}{\partial r} \delta h = - \delta E \left[\beta\gamma \frac{d\gamma}{dr} + \frac{4\beta\gamma^2}{r} \right] \qquad \text{(A.5)}$$

$$+ \delta h \left[\beta\gamma^2 \frac{d\beta}{dr} - \frac{H_r^2}{4\pi\rho^* c^2 r} + \frac{3\gamma^2\beta^2}{r} + \gamma\beta^2 \frac{d\gamma}{dr} \right]$$

Equation (II.22) is our second equation for δh and δE, and has the form

$$\frac{1}{c} \frac{\partial}{\partial t} \delta h + \frac{\partial}{\partial r} \delta E = - \frac{\delta E}{r} \qquad \text{(A.6)}$$

We now apply the method described by Weinberg (1962) to obtain the WKB amplitudes (see also Belcher 1971b). Let L be the scale height for variations in ρ^*, β, and H_r. We write δE and δh in the form

$$\delta E(r,t) = [\delta E_1(r) + \mu \delta E_2(r) + \mu^2 \delta E_3(r) + \ldots] \exp[i(\omega t - S(r)]$$

$$\delta h(r,t) = [\delta h_1(r) + \mu \delta h_2(r) + \mu^2 \delta h_3(r) + \ldots] \exp[i(\omega t - S(r)] \qquad \text{(A.7)}$$

where

$$k = \frac{dS}{dr} \qquad \mu = \frac{2\pi}{kL} \qquad \text{(A.8)}$$

The parameter μ is the ratio of the wavelength to the scale height L, and is assumed to be small. The quantities δE_1, δE_2, δh_1, etc., are also assumed to have scale heights on the order of L. We insert equation (A.7) into equations (A.5) and (A.6), and keep only terms to first order in μ . If we place zeroth order terms in μ on the left hand side, and first order terms on the right hand side, we obtain the equations

$$- \frac{i\omega}{c} \delta h_1 + ik \delta E_1 = - \mu \left[- \frac{i\omega}{c} \delta h_2 + ik \delta E_2\right] - \frac{\delta E_1}{r} - \frac{d}{dr} \delta E_1 \tag{A.9}$$

and

$$- \frac{i\omega}{c} \left(\gamma^2 + \frac{H_r^2}{4\pi\rho^* c^2 \eta}\right) \delta E_1 + i2\gamma^2 \beta k \, \delta E_1$$

$$+ ik \left(\frac{\eta H_r^2}{4\pi\rho^* c^2} - \beta^2\gamma^2\right) \delta h_1 = - \mu \left[- \frac{i\omega}{c} \left(\gamma^2 + \frac{H_r^2}{4\pi\rho^* c^2 \eta}\right) \delta E_2\right.$$

$$\left. + i2\gamma^2 \beta k \, \delta E_2 + ik \left(\frac{\eta H_r^2}{4\pi\rho^* c^2} - \beta^2\gamma^2\right) \delta h_2\right]$$

$$+ \delta h_1 \left[\beta\gamma^2 \frac{d\beta}{dr} - \frac{H_r^2}{4\pi\rho^* c^2 r} + \frac{3\gamma^2\beta^2}{r} + \gamma\beta^2 \frac{d\gamma}{dr}\right]$$

$$- \delta E_1 \left[\beta\gamma \frac{d\gamma}{dr} + \frac{4\beta\gamma^2}{r}\right] - 2\gamma^2\beta \frac{d}{dr} \delta E_1$$

$$- \left(\frac{\eta H_r^2}{4\pi\rho^* c^2} - \beta^2\gamma^2\right) \frac{d}{dr} \delta h_1 \tag{A.10}$$

where we have assumed that $r \gtrsim L$. The zeroth-order approximation is obtained by assuming the right hand sides of (A.9) and (A.10) are zero. Using β_a as defined by equation (II.26), we find that

$$\beta_p = \frac{\omega}{ck} = \frac{\beta + \eta\beta_a}{1 + \beta\beta_a/\eta} \tag{A.11}$$

and

$$\delta h_1 = \frac{\delta E_1}{\beta_p} \tag{A.12}$$

We have chosen the sign in equation (A.11) for outwardly propagating waves.

To obtain the first-order solutions, we insert the zeroth order solutions (A.11) and (A.12) into equations (A.9) and (A.10). To eliminate the quantities δE_2 and δh_2, we then multiply equation (A.9) by $(\eta H_r^2/4\pi\rho^* c^2 - \beta^2\gamma^2)/\beta_p$ and add it to equation (A.10). This leaves us with a differential equation for δE_1 of the form

$$\frac{1}{\beta_p r}\left(\frac{\beta_a^2\eta}{1-\beta_a^2} - \beta^2\gamma^2\right)\frac{d}{dr}(r\delta E_1) + 2\gamma^2\beta\frac{d}{dr}\delta E_1$$

$$+ \left(\frac{\eta\beta_a^2}{1-\beta_a^2} - \beta^2\gamma^2\right)\frac{d}{dr}\left(\frac{\delta E_1}{\beta_p}\right) + \delta E_1\left(\beta\gamma\frac{d\gamma}{dr} + \frac{4\beta\gamma^2}{r}\right)$$

$$- \frac{\delta E_1}{\beta_p}\left(\beta\gamma^2\frac{d\beta}{dr} - \frac{\beta_a^2}{1-\beta_a^2}\frac{1}{r} + \frac{3\gamma^2\beta^2}{r} + \gamma\beta^2\frac{d\gamma}{dr}\right) = 0 \tag{A.13}$$

To solve equation (A.13), we write all derivatives of the form $d\beta/dr$, $d\gamma/dr$, $d\beta_a/dr$, and so on, in terms of $d\rho^*/dr$. For example, we have from equation (A.1) that

$$\frac{d\gamma}{dr} = \gamma^3 \left[\frac{\beta}{\eta} \frac{d\beta}{dr} - \frac{1}{2} \left(1 + \frac{\beta^2}{\eta^2}\right) \frac{d\eta}{dr} \right] \tag{A.14}$$

We also have [cf. equation (II.18)]

$$\frac{2}{r} + \frac{1}{\rho^*} \frac{d\rho^*}{dr} + \frac{1}{\gamma} \frac{d\gamma}{dr} + \frac{1}{\beta} \frac{d\beta}{dr} = 0 \tag{A.15}$$

From (A.14) and (A.15) we can obtain expressions for $d\beta/dr$ and $d\gamma/dr$ in terms of $d\rho^*/dr$ alone. From the definition of β_a, we also can obtain an expression for $d\beta_a/dr$ in terms of $d\rho^*/dr$ [cf. equation (II.43)]. Proceeding in this manner, we eliminate all derivatives in equation (A.13) except those of ρ^* and δE_1. After a tedious process, we obtain the equation

$$\frac{1}{\delta E_1} \frac{d}{dr} \delta E_1 = - \frac{1 - \beta_a^2}{4 \rho^*} \frac{d\rho^*}{dr} + \frac{\beta_a^2 - 2}{r} \tag{A.16}$$

The solution to this equation is (II.29). We obtain expressions for the radial dependence of δH_1 and $\delta\beta_1$ by using equation (II.29) in conjunction with equations (A.3), (A.4) and (A.12).

Appendix B

We sketch a derivation of the non-relativistic equation (II.48) in the limit that β and β_e are small compared to one, with no restrictions on β_a. The possibility that β_a may be close to one means that we must keep time derivatives of $\underset{\sim}{E}$ in Maxwell's equations. For a non-relativistic MHD plasma with fluid velocity $\underset{\sim}{V}$, density ρ, magnetic field $\underset{\sim}{H}$, and electric field $\underset{\sim}{E}$, in the presence of a spherically symmetric gravitational potential Φ, the relevant equations are

$$\rho \frac{D}{Dt} \underset{\sim}{V} + \underset{\sim}{\nabla} p + \rho \underset{\sim}{\nabla} \Phi + \frac{1}{4\pi} \underset{\sim}{H} \times \left[\underset{\sim}{\nabla} \times \underset{\sim}{H} - \frac{1}{c} \frac{\partial}{\partial t} \underset{\sim}{E} \right] = 0 \tag{B.1}$$

$$\underset{\sim}{\nabla} \times \underset{\sim}{E} + \frac{1}{c} \frac{\partial}{\partial t} \underset{\sim}{H} = 0 \tag{B.2}$$

$$\underset{\sim}{E} + \frac{1}{c} \underset{\sim}{V} \times \underset{\sim}{H} = 0 \tag{B.3}$$

If we assume that $\underset{\sim}{V} = V(r)\hat{e}_r + \delta V(r,t)\hat{e}_\phi$ and $\underset{\sim}{H} = H(r)\hat{e}_r + \delta H(r,t)\hat{e}_\phi$, then from equation (B.3) we immediately have $\underset{\sim}{E} = \delta E(r,t)\hat{e}_\theta$, with $\delta E = (V\delta H - H\delta V)/c$. The ϕ-component of equation (B.1) is

$$\frac{\partial}{\partial t} \delta V + \frac{V}{r} \frac{\partial}{\partial r} (r\delta V) = \frac{H}{4\pi\rho r} \frac{\partial}{\partial r} (r\delta H) + \frac{H}{4\pi\rho c} \frac{\partial}{\partial t} \delta E \tag{B.4}$$

The ϕ-component of equation (B.2) is

$$\frac{1}{c}\frac{\partial}{\partial t}\,\delta H + \frac{1}{r}\frac{\partial}{\partial r}\,(r\delta E) \;=\; 0 \tag{B.5}$$

Thus, our perturbation quantities satisfy equations which are the non-relativistic limits of equations (II.21), (II.22), and (II.24). Hence, the WKB solutions to equations (B.4) and (B.5) are the non-relativistic limits of the solutions given by equations (II.27) through (II.32). For convenience, we now assume our perturbations are circularly polarized in the equatorial plane of a spherical polar coordinate system.

The radial component of equation (B.1) may be written as

$$V\frac{dV}{dr} - \frac{\delta V^2}{r} + \frac{1}{\rho}\frac{dp}{dr} + \frac{d\Phi}{dr} + \frac{1}{4\pi\rho c}\frac{\partial}{\partial t}\,(\underset{\sim}{E}\times\underset{\sim}{H})_r$$

$$+\;\frac{1}{4\pi\rho}\left\{\underset{\sim}{H}\times(\underset{\sim}{\nabla}\times\underset{\sim}{H}) + \underset{\sim}{E}\times(\underset{\sim}{\nabla}\times\underset{\sim}{E})\right\}_r \;=\; 0 \tag{B.6}$$

where we have used equation (B.2). Our assumption of circular polarization implies that $\underset{\sim}{E}\times\underset{\sim}{H}$ is time-independent, so that equation (B.6) becomes

$$V\frac{dV}{dr} + \frac{1}{\rho}\frac{dp}{dr} + \frac{d\Phi}{dr} + \frac{1}{r\rho}\left[\frac{1}{4\pi}\,(\delta H^2 + \delta E^2) - \rho\delta V^2\right]$$

$$+\;\frac{1}{8\pi\rho}\frac{d}{dr}\left[\delta H^2 + \delta E^2\right] \;=\; 0 \tag{B.7}$$

We may write equation (B.7) in terms of $d\beta/dr$ alone by using the conservation of mass and equation (II.29) for the radial dependences of the transverse perturbations in terms of ρ, V, and r. In particular, we note that in this limit

$$\frac{d\beta_p}{dr} = \frac{(1 - \beta_a^2)}{(1 + \beta\beta_a)^2} \left[\frac{1}{2\beta} \frac{d\beta}{dr} (2\beta + \beta_a) - \frac{\beta_a}{r}\right] \qquad \text{(B.8)}$$

After some tedious manipulations, we recover equation (II.48) for dV/dr, neglecting third order terms in small quantities.

References

Alazraki, G., and Couturier, P. 1971, Astr. and Ap., 13, 380.

Barnes, A. 1973, in Advances in Electronics and Electron Physics (Academic Press), L. Marton, ed.

Barnes, A., and Suffolk, G. 1971, J. Plasma Phys., 5, 315.

Barnes, A., and Hollweg, J. V. 1973, J Geophys. Res., in press.

Belcher, J. 1971, Ap. J., 168, 509.

Belcher, J. 1972, Solar Wind, edited by C. P. Sonnett, P. J. Coleman, and J. M. Wilcox, NASA SP-308, p. 382.

Belcher, J., Davis, L., and Smith, E. J. 1969, J. Geophys. Res., 74, 2302.

Belcher, J., and Davis, L. 1971, J. Geophys. Res., 76, 3534.

Coleman, P. J., Jr. 1967, Plan. Space Sci., 15, 953.

Greenberg, P. 1971, Ap. J., 164, 589.

Harris, E. 1957, Phys. Rev., 108, 1357.

Hollweg, J. V. 1972, Cosmic Electrodyn., 2, 423.

Hollweg, J. V. 1973a, Ap. J., 181, 547.

Hollweg, J. V. 1973b, J. Geophys. Res., 78, 3643.

Hundhausen, A. J. 1972, Coronal Expansion and the Solar Wind (New York, Springer-Verlag).

Landau, L. and Lifshitz, E. 1971, Classical Theory of Fields (New York, Pergamon Press).

Møller, A. 1952, Theory of Relativity (Oxford, Clarendon Press).

Parker, E. N. 1965, Space Sci. Rev., 4, 666.

Parker, E. N. 1971, Rev. Geophys. and Space Phys., 9, 825.

Unti, T., and Neugebauer, M. 1968, Phys. Fluids, 11, 563.

Weinberg, S. 1962, Phys. Rev., 126, 1899.

Whang, Y. C. 1973, J. Geophys. Res., in press.

FIGURE CAPTIONS

Figure 1. Critical point solutions (r_c/r_o, β_c/β_{eo}, β_o/β_{eo}) as functions of $\delta\beta_o^2/\beta_{eo}^2$ for values of $\beta_{so}^2/\beta_{eo}^2$ equal to 0.1, 0.040, and 0.001 (curves labeled A, B, and C, respectively). The Alfvén velocity $c\beta_{ao}$ and the escape velocity $c\beta_{eo}$ are constant, with $\beta_{ao} = 0.0001$ and $\beta_{eo} = 0.0020$. The limiting velocity of the wind at infinity is $c\beta_\infty$. The dotted curves represent analytic results derived in Section IV under various approximations (see text). The scale for r_c/r_o is to the right and the scale for all other quantities is to the left.

Figure 2. Energy flux and mass flux as functions of $\delta\beta_o^2/\beta_{eo}^2$ for the same values of $\beta_{so}^2/\beta_{eo}^2$, β_{ao}, and β_{eo} as in Figure 1. We also plot $F_E/c^2F_M - 1$, which is $\gamma_\infty - 1$.

Figure 3. The curves labeled 1 through 4 correspond to the values of $\delta\beta_o^2/\beta_{eo}^2$ indicated on curve A of β_o/β_{eo} in Figure 1. The curves labeled 5 are for a value of $\delta\beta_o^2/\beta_{eo}^2$ indicated by a vertical stub on the axis in Figure 1 (this point is below the cutoff for dynamic solutions). The quantity $\beta_{so}^2/\beta_{eo}^2$ is 0.1, with $\beta_{ao} = 0.0001$ and $\beta_{eo} = 0.0020$. We plot different variables as functions of radial distance from the

reference level r_o: (a) The mass density normalized to its value at r_o, and the radial streaming velocity divided by the escape velocity at r_o; (b) The Alfvén velocity divided by c, and the transverse velocity divided by the Alfvén velocity; (c) The transverse velocity divided by the escape velocity at r_o, and the transverse velocity divided by the radial velocity. (d) The Alfvén wave energy flux A normalized to its value at r_o, and the radial Alfvénic mach number. The scales for the various quantities are to the left or to the right, as indicated. Vertical stubs on the curves indicate the location of the critical points.

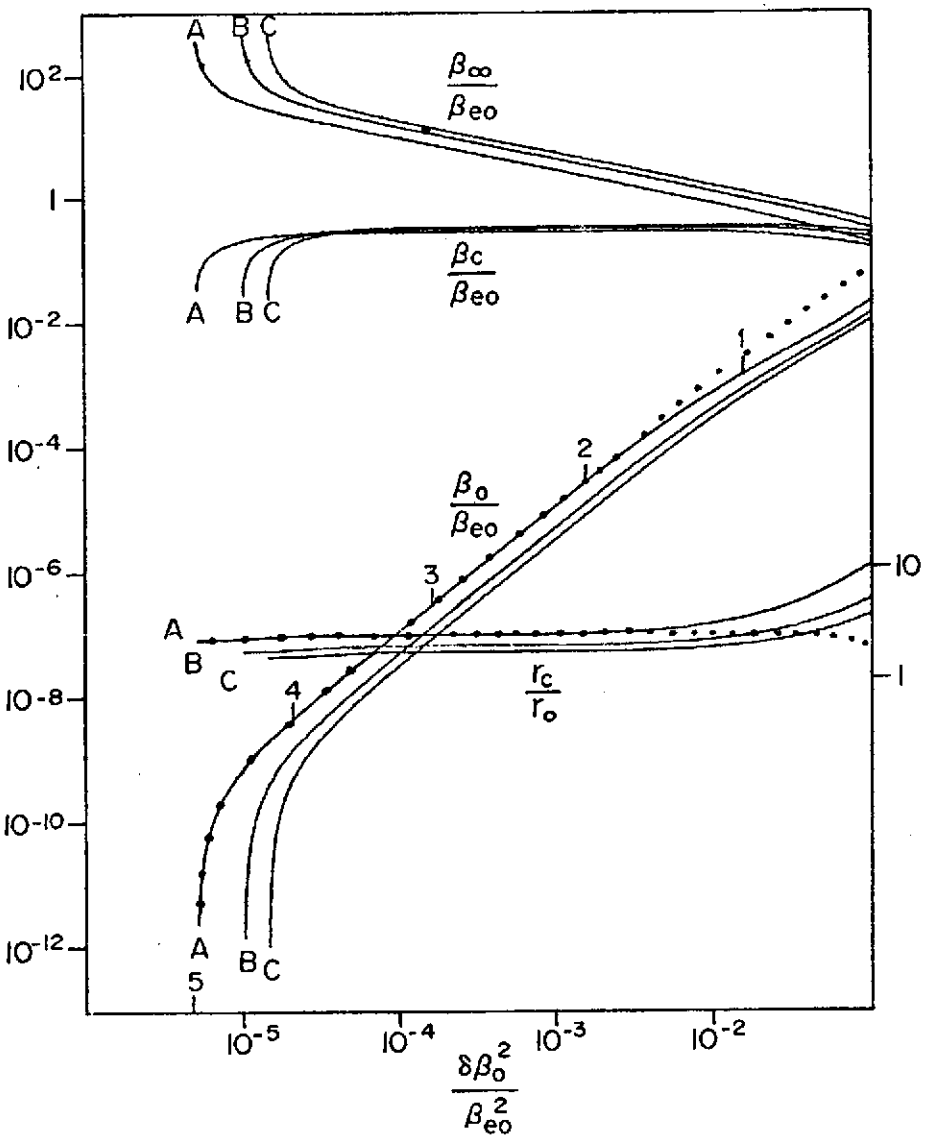
A B C
$\frac{\beta_\infty}{\beta_{eo}}$
$\frac{\beta_c}{\beta_{eo}}$
$\frac{\beta_o}{\beta_{eo}}$
$\frac{r_c}{r_o}$
10^2
1
10^{-2}
10^{-4}
10^{-6}
10^{-8}
10^{-10}
10^{-12}
10
1
1
2
3
4
5
10^{-5}
10^{-4}
10^{-3}
10^{-2}
$\frac{\delta\beta_o^2}{\beta_{eo}^2}$

FIGURE 1

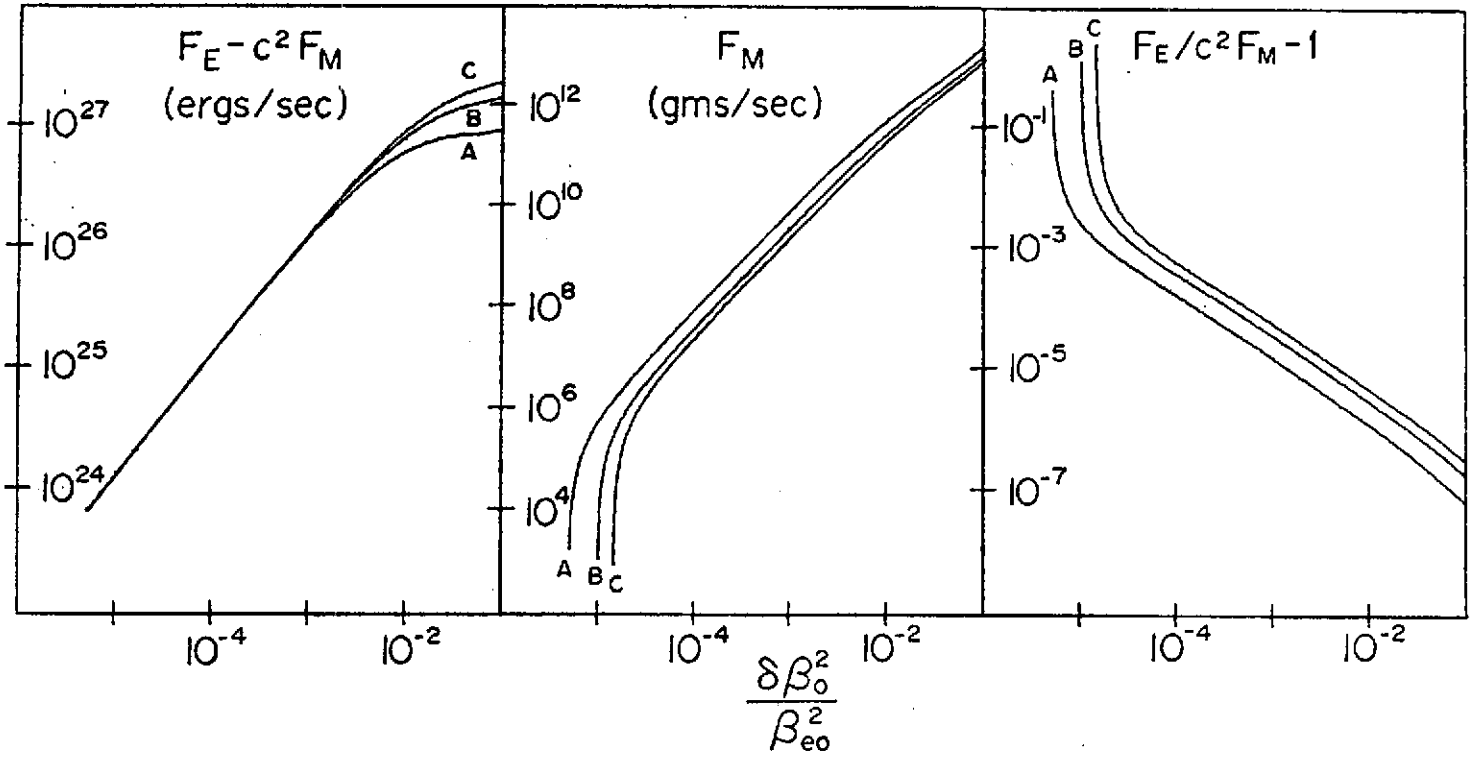
$F_E - c^2 F_M$
(ergs/sec)
10^{27}
10^{26}
10^{25}
10^{24}
C
B
A
10^{-4}
10^{-2}
F_M
(gms/sec)
10^{12}
10^{10}
10^{8}
10^{6}
10^{4}
A
B
C
10^{-4}
10^{-2}
$\frac{\delta\beta_o^2}{\beta_{eo}^2}$
$F_E/c^2 F_M - 1$
A
B
C
10^{-1}
10^{-3}
10^{-5}
10^{-7}
10^{-4}
10^{-2}

FIGURE 2

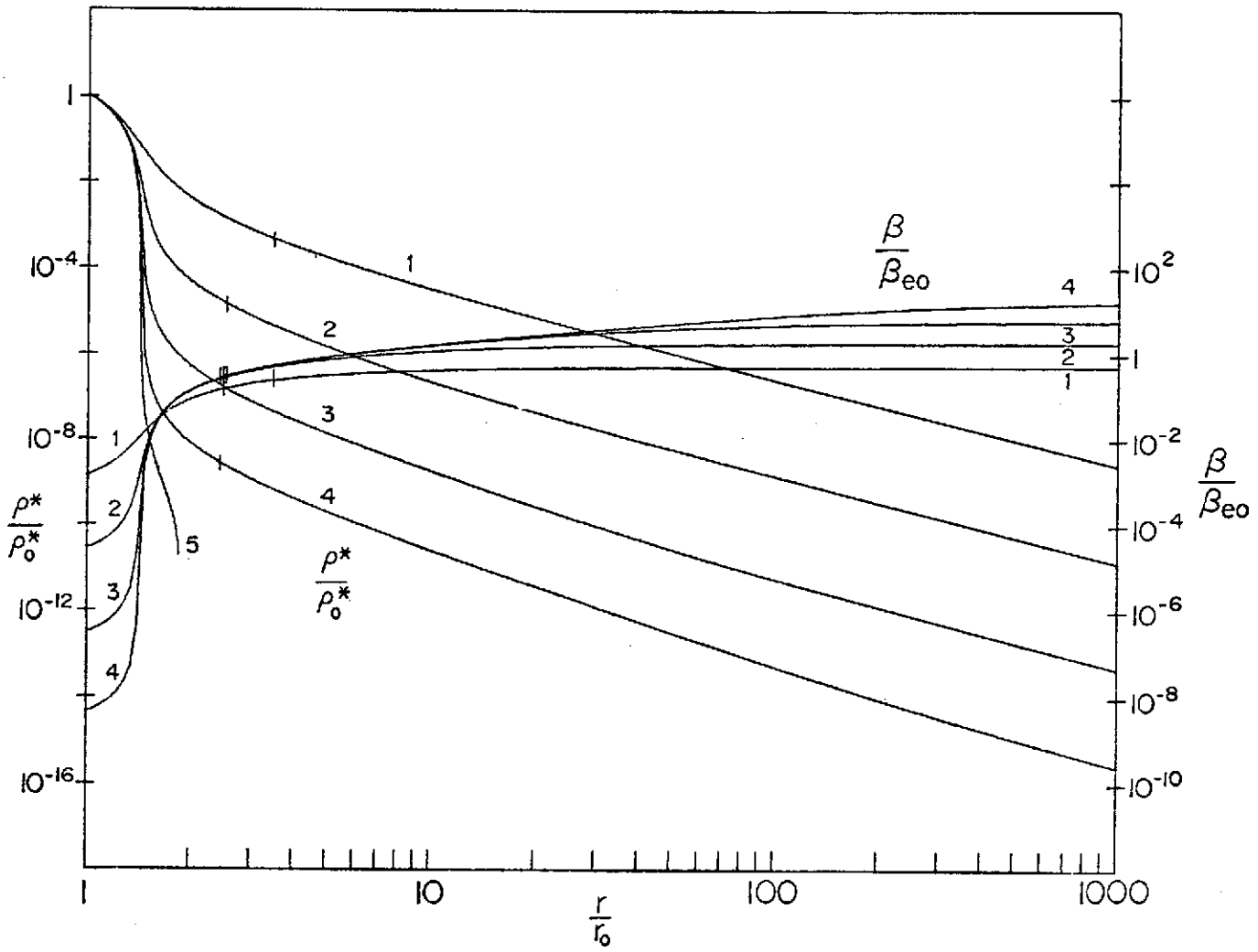
1
10^{-4}
10^{-8}
10^{-12}
10^{-16}
$\frac{\rho^*}{\rho_0^*}$
1
2
3
4
5
$\frac{\beta}{\beta_{eo}}$
1
2
3
4
$\frac{\rho^*}{\rho_0^*}$
10^2
1
10^{-2}
10^{-4}
10^{-6}
10^{-8}
10^{-10}
$\frac{\beta}{\beta_{eo}}$
1
10
100
1000
$\frac{r}{r_0}$

FIGURE 3a

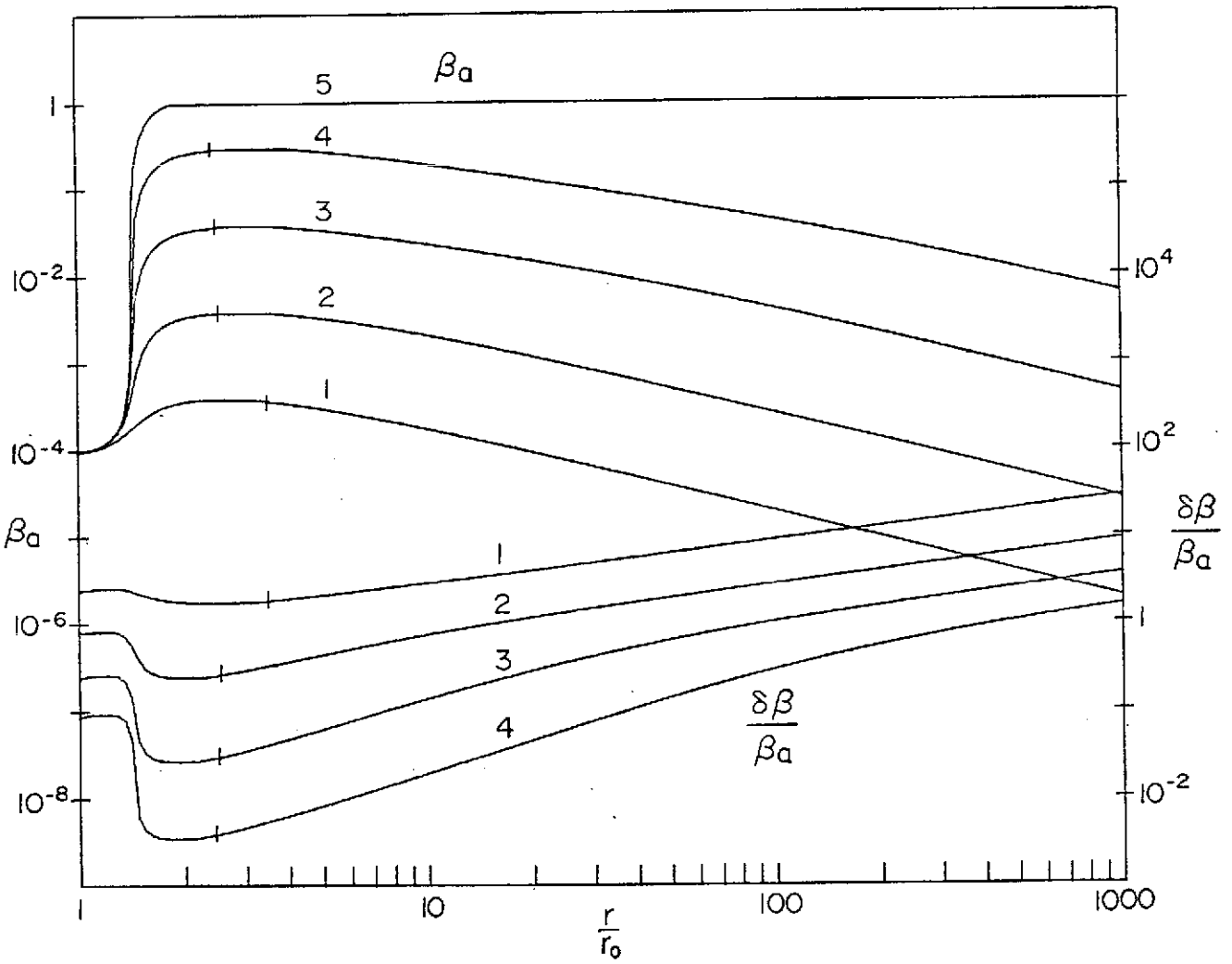
β_a
5
4
3
2
1
1
10^{-2}
10^{-4}
10^{-6}
10^{-8}
β_a
1
2
3
4
$\frac{\delta\beta}{\beta_a}$
10^4
10^2
1
10^{-2}
$\frac{\delta\beta}{\beta_a}$
1
10
100
1000
$\frac{r}{r_o}$

FIGURE 3b

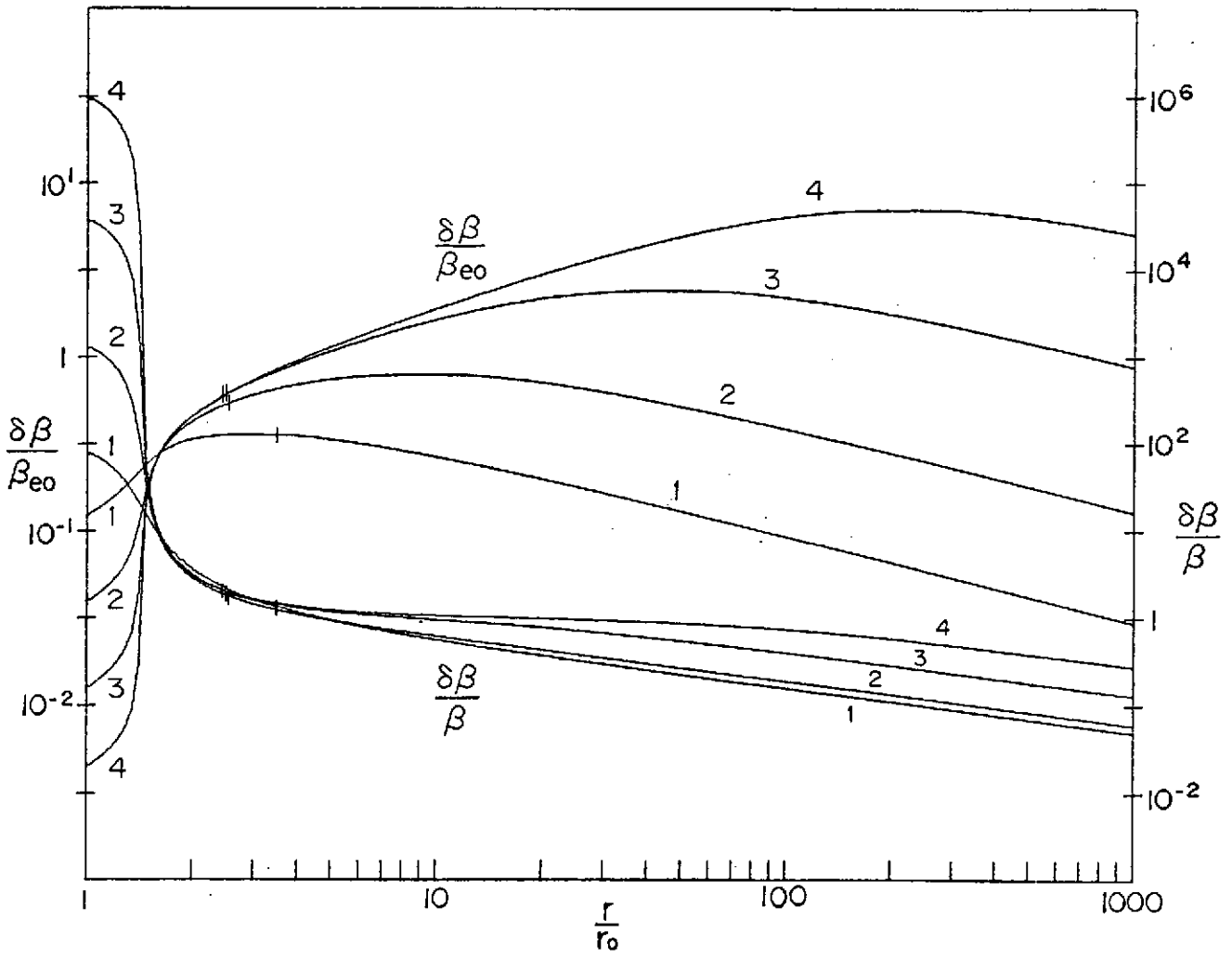
$\frac{\delta\beta}{\beta_{eo}}$
$\frac{\delta\beta}{\beta}$
$\frac{r}{r_o}$
10¹
1
10⁻¹
10⁻²
10⁶
10⁴
10²
1
10
100
1000
4
3
2
1

FIGURE 3c

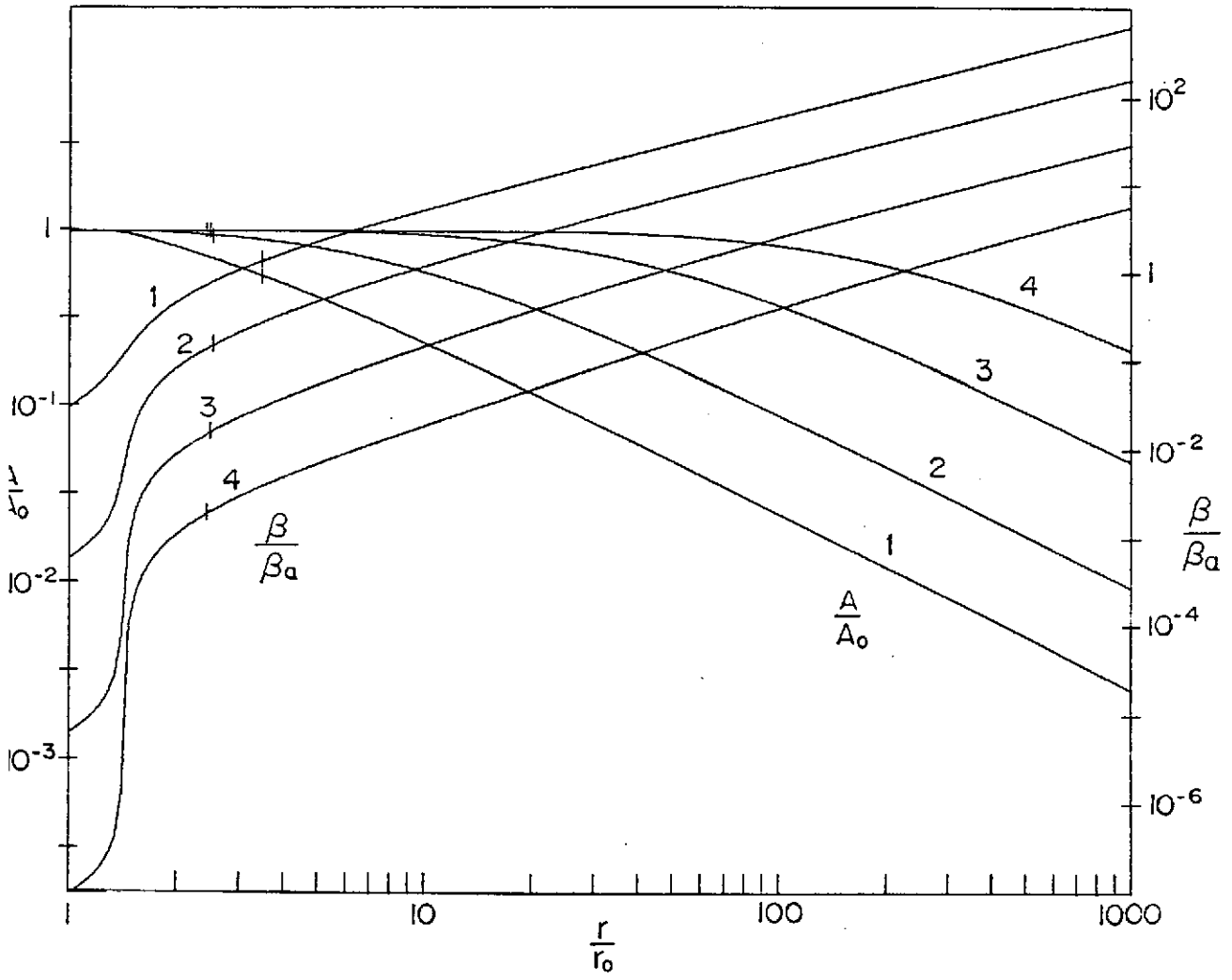
1
10^{-1}
10^{-2}
10^{-3}
$\frac{\lambda}{\lambda_0}$
$\frac{\beta}{\beta_a}$
1
2
3
4
$\frac{A}{A_0}$
10^2
1
10^{-2}
10^{-4}
10^{-6}
$\frac{\beta}{\beta_a}$
1
10
100
1000
$\frac{r}{r_0}$

FIGURE 3d